

Integrated Quantum Nanophotonics with Solution-Processed Materials

Yueyang Chen, David Sharp, Abhi Saxena, Hao Nguyen, Brandi M. Cossairt, and Arka Majumdar*

A key obstacle for all quantum information science and engineering platforms is their lack of scalability. The discovery of emergent quantum phenomena and their applications in active photonic quantum technologies have been dominated by work with single atoms, self-assembled quantum dots, or single solid-state defects. Unfortunately, scaling these systems to many quantum nodes remains a significant challenge. Solution-processed quantum materials are uniquely positioned to address this challenge, but the quantum properties of these materials have remained generally inferior to those of solid-state emitters or atoms. Additionally, systematic integration of solution-processed materials with dielectric nanophotonic structures has been rare compared to other solid-state systems. Recent progress in synthesis processes and nanophotonic engineering, however, has demonstrated promising results, including long coherence times of emitted single photons and deterministic integration of emitters with dielectric nano-cavities. In this review article, these recent experiments using solution-processed quantum materials and dielectric nanophotonic structures are discussed. The progress in non-classical light state generation, exciton-polaritonics for quantum simulation, and spin-physics in these materials is discussed and an outlook for this emerging research field is provided.

1. Introduction

The field of quantum information science and engineering (QISE) has entered a new era. Hundreds of academic research groups, national laboratories, and even high-tech companies are racing to build machines that can tackle classically intractable

computing and simulation problems, as well as, revolutionize communications and cryptography.^[1] These quantum processors are built using various physical systems, among which superconducting circuits, and trapped ions are leading candidates. However, despite recent impressive proof-of-concept devices, such as, Google's 53-qubit Sycamore,^[2] IonQ,^[3,4] Honeywell,^[5] and IBM Q, the road to a practical, fault-tolerant quantum computer remains full of challenges due to the inherent fragility of quantum states. In fact, protecting these fragile quantum states from detrimental external noise remains an ongoing struggle. Moreover, a useful quantum computer will need millions of qubits, which can possibly be realized only in a distributed quantum computing system,^[6,7] where a few (≈ 50) qubit quantum computers will be connected to each other in a network. This necessitates interfacing with quantum communication systems, which are predominantly based on photonic qubits. Hence the quantum states need to be transduced to optical photons without adding substantial

noise, a difficult feat on its own.^[8] By contrast, photonic qubit systems have several unique advantages:^[9] Quantum states of photons are easily preserved due to their extremely weak interaction with the external environment, photons can maintain their coherence at room temperature and photonic quantum computers are completely compatible with quantum communication as the qubits are already realized using photons. In fact, two recent demonstrations of photonic quantum computers (Xanadu^[10] and Jiuzhang^[11]) show the immense potential of photonics for QISE. However, the scalability of these photonic quantum computers remains an extremely challenging problem, due to lack of quantum light sources and quantum nonlinearity as well as efficient, coherent interfacing with matter qubits.

While the noisy intermediate-scale quantum-era could be realized using photonic qubits, an extremely large number of resources are needed to create a fully fault-tolerant quantum computer. Relying on linear optics would be even more resource intensive,^[12] and integrated photonics seem to be the only viable route.^[13] In fact, very-large-scale integration is indeed possible in silicon (and in recent years in silicon nitride) photonics using CMOS foundries. **Figure 1a** shows a multidimensional quantum entanglement platform enabled by large-scale silicon integrated

Y. Chen, A. Saxena, A. Majumdar
Department of Electrical and Computer Engineering
University of Washington
Seattle, WA 98195, USA
E-mail: arka@uw.edu

D. Sharp, A. Majumdar
Department of Physics
University of Washington
Seattle, WA 98195, USA

H. Nguyen, B. M. Cossairt
Department of Chemistry
University of Washington
Seattle, WA 98195, USA

 The ORCID identification number(s) for the author(s) of this article can be found under <https://doi.org/10.1002/qute.202100078>

DOI: 10.1002/qute.202100078

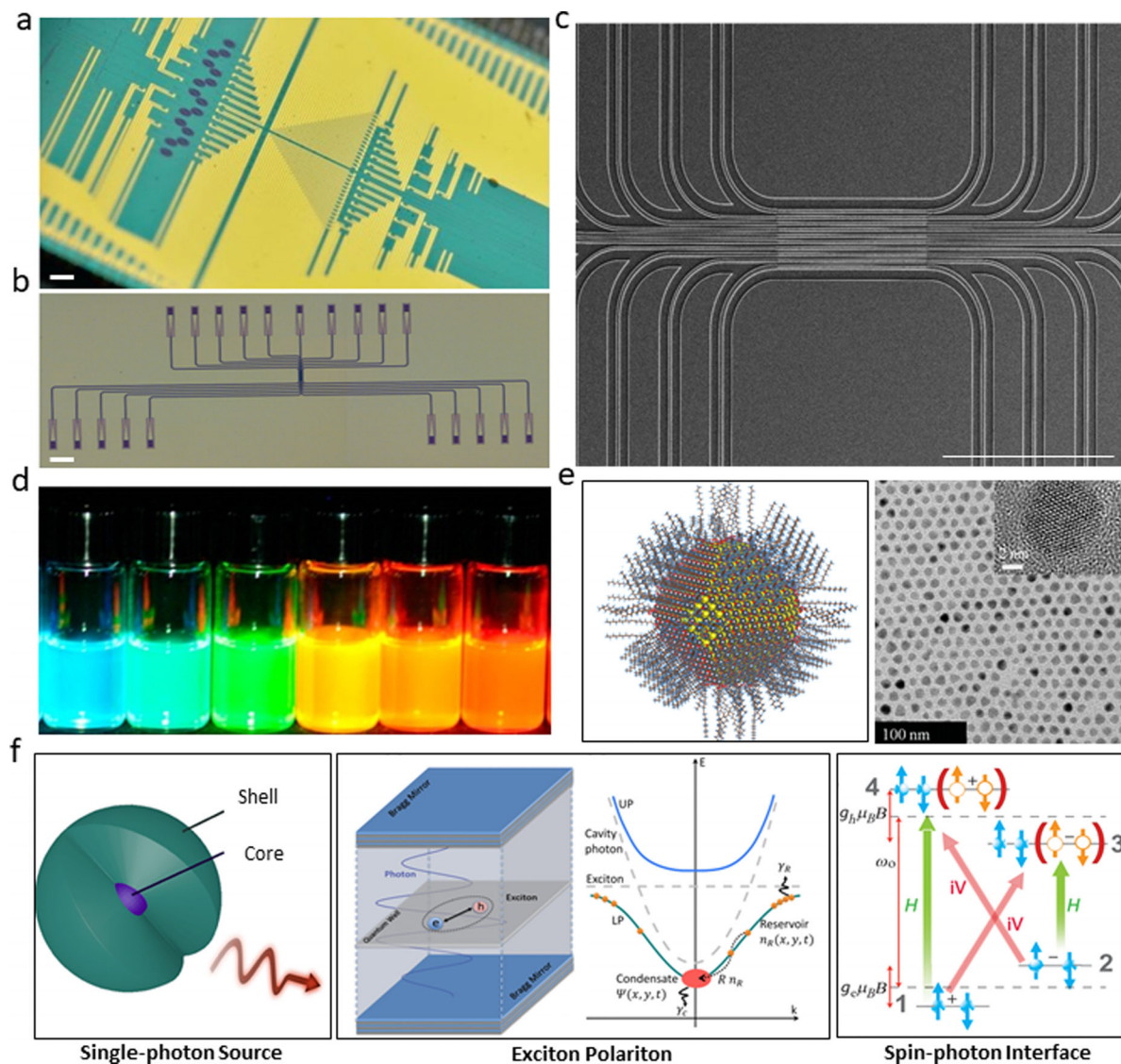


Figure 1. Paper outline. a) Scalable silicon quantum photonics circuits: Multidimensional quantum photonic platform able to generate, control, and analyze high-dimensional entanglement^[14] (scale bar: 1 mm). b) Microscope image of many coupled photonic crystal cavities, fabricated by state-of-art ebeam lithography with subwavelength precision (scale bar: 50 μm). c) Scanning electron microscopy (SEM) images of the photonic crystal cavities (scale bar: 50 μm). d) Solution-processed materials are efficient light emitters that support room-temperature operation over a broad and tailorable spectral range.^[59] e) A computational model of a solution-processed QD^[43] and an experimental transmission electron microscope (TEM) image.^[44] Different robust wet-chemical techniques have been explored for synthesis of the QDs, and their stability and performance are typically improved by a core-shell structure with organic ligands attached on the surface. f) Quantum nanophotonics applications of solution-processed material: Single-photon source;^[60] Exciton Polaritons;^[61] Spin-photon interface.^[62] Figures are reprinted with permission: a) Reproduced with permission.^[14] Copyright 2018, AAAS. d) Reproduced with permission.^[59] Copyright 2015, American Chemical Society. e) Left panel, Reproduced with permission.^[43] Copyright 2014, AAAS; Right panel, Reproduced with permission.^[44] Copyright 2015, Wiley-VCH. f) Left panel, Reproduced with permission.^[60] Copyright 2017, American Chemical Society; Middle panel, Reproduced with permission.^[61] Copyright 2016, American Physical Society; Right panel, Reproduced with permission.^[62] Copyright 2013, American Physical Society.

photonics.^[14] However, creating large-scale on-demand quantum light sources on silicon photonics platforms remains challenging. For example, III–V self-assembled quantum dots (QDs) have been extensively studied for single-photon emission,^[15–21] yet integrating III–V materials on a silicon-compatible platform is not straightforward.^[22] Additionally, self-assembled QDs suffer from random spatial positioning and inhomogeneous spectral broadening. To overcome the random positioning problem, ef-

forts have been made on site-controlled growth of QDs, yet such methods are always accompanied by inferior quantum-optical properties due to the surface roughness of the pre-patterned nanoholes.^[23] In situ optical lithography and electron beam lithography has recently attracted attention since they only require a quick surface scan to locate the quantum emitter with pristine optical property.^[24,25] However, such post-growth selection method does not mitigate the random positioning nature

of the self-assembled QDs, making the creation of large arrays of quantum emitters difficult. In recent years, new techniques such as “pick-and-place” have attracted more attentions, but they still require complicated nano-fabrication processes.^[26,27] Various tuning mechanisms have also been explored to mitigate inhomogeneous broadening, including tuning via temperature control,^[28] strain engineering,^[29,30] electrical and magnetic fields.^[31–33] However, challenges remain as the achievable tuning range is only a fraction of the whole inhomogeneous broadening scale.^[27] Instead of linear optical quantum computing, quantum nonlinearity at the single-photon level could potentially reduce a large number of resources.^[34,35] By coupling a single self-assembled QD to an integrated photonic crystal cavity, single photon nonlinearity has also been experimentally demonstrated.^[36,37] But engineering such nonlinear interaction in a scalable fashion, again, remains very difficult. While state-of-the-art fabrication methods can yield many photonic crystal cavities with subwavelength precision (Figure 1b,c), large-scale control over the positioning of multiple QDs remains elusive. Finally, the spin-photon interface in solid-state systems is a critical resource for quantum repeaters and quantum communication. While significant progress has been made on this front using spin-states hosted in defect centers, including, NV and SiV centers in diamond,^[38] SiV centers in SiC,^[39] and rare-earth doped materials,^[40] creating a large network is still limited by a multitude of material issues.^[41]

Solution-processed quantum materials could potentially provide a novel approach to solve these long-standing problems and provide a route to scalability.^[42] As shown in Figure 1d, they are efficient quantum light emitters that support room-temperature operation over a broad and tailorable spectral range. Figure 1e shows a computational model of a solution-processed QD^[43] and an experimental transmission electron microscope image.^[44] Different robust wet-chemical techniques have been explored for synthesis of the QDs, and their stability and performance are typically improved by a core-shell structure with organic ligands attached on the surface. Colloidal synthesis can produce ultra-high purity nanocrystalline materials, that is, materials with an extremely low background of unintentional dopants, as compared to epitaxial growth,^[45] as well as, complex heterostructures with engineered quantum confinement of electrons and holes. The synthetic control over growing materials with atomistic precision provides an interesting opportunity to engineer quantum properties.^[46] Moreover, these materials can be easily integrated with any substrate via solution-phase processing methods like spin-coating, making them an excellent candidate for creating silicon or silicon nitride-based quantum photonic systems. Unfortunately, colloidal quantum emitters have suffered in the past from problems, such as, material instability under ambient conditions and broadened emission linewidths due to non-radiative decay and spectral wandering. However, recent progress in synthesis techniques have solved some of these problems,^[47] and further improvements are possible. We note that to date, the primary research focus for colloidal emitter systems had been in the area of wide color gamut displays and solid-state lighting,^[48,49] and not for QISE. Thus, engineering these emitters for quantum applications remains underexplored. Finally, the ease of integration of solution-processed materials to nanophotonic structures (i.e., by drop-casting or spin-coating) provides an excellent

opportunity to engineer strong light-matter interactions, thanks to the temporal and spatial confinement of light.

In this paper, we review the recent progress in integrated quantum nanophotonics using solution-processed materials. Specifically, we explore non-classical light generation, including single-photon emission and nano-lasing, exciton-polaritonics for quantum simulation and spin-physics within these material systems (Figure 1f). We also highlight the outstanding challenges and potential future research directions for quantum nanophotonics with solution-processed materials. We note that a large body of work on solution-processed materials coupled to plasmonic nanostructures exists. However, in this review, we primarily focus on dielectric nano-photonic structures because of their low optical loss, and ability to create large-scale integrated photonic circuits. Specifically, we focus on two distinct types of nano-resonators: i) low-mode volume resonators with 3D confinement of light, and ii) resonators supporting delocalized resonant modes with light tightly confined in only one dimension. An example of the first type, also called 0D cavities are photonic crystal defect mode cavities, such as, linear three hole (L3) defect cavities^[50] or nanobeam resonators.^[51] The second type, also known as 2D cavities include distributed Bragg reflector (DBR) cavities,^[52] and guided mode resonators/nonlocal metasurfaces.^[53,54] 0D cavities can provide ultra-small sub-wavelength mode volume and thus can provide extremely large light-matter interaction strength. However, tuning these cavities is difficult, and one needs to resort to gas tuning,^[55,56] or thermal tuning.^[57,58] Both mechanisms provide a very limited tuning range and may not be suitable to demonstrate strong coupling with broad solution-processed emitters. The resonance wavelength of 2D cavities, on the other hand, can be easily tuned by collecting light at different angles, due to the dispersive nature of these cavities. Hence, this type of 2D cavity is often preferred to study exciton-polaritonics.

2. Non-Classical Light Generation

One of the most important resources for photonic QISE is non-classical light sources. These sources emit light that does not obey classical photon statistics. Among them, single-photon sources are the most heavily investigated, and form the basis of many other non-classical states, such as, Bell states or NOON states.^[63]

2.1. Single-Photon Sources

Single-photon sources play a crucial role in quantum networks,^[64] and universal linear quantum computing,^[10,65] including boson sampling.^[66] A good single-photon source needs to satisfy three criteria: i) efficient multi-photon suppression, that is, the emitted light has no multi-photon state, signified by second-order autocorrelation $g^{(2)}(0)$ to be zero (measured using a Hanbury Brown Twiss setup); ii) high indistinguishability, that is, the emitted photons are identical, as measured by a dip in coincidence count in a Hong–Ou–Mandel (HOM) measurement; and iii) high rate of generation. While a large number of quantum experiments rely on spontaneous parametric down-converted single photons, the rate of such

photon generation is low (≈ 10 's of MHz).^[67] By using solid-state quantum emitters, such as, self-assembled QDs, this rate can be increased to GHz.^[68] While single photons emitted from QDs have long suffered from poor indistinguishability and low purity, with continuous engineering, and by exploiting Purcell enhancement via cavity integration, indistinguishable, pure single photon emission has been demonstrated and used in boson sampling experiments.^[69,70] It is worth pointing out that it took almost 20 years for QD single photon sources^[16–18] to be used in large-scale quantum experiments.^[69,70] Even there, only a single QD source is used, and the emitted photons are time-multiplexed for interferometry.^[69,70] Looking at the vast resources needed for photonic QISE, it is imperative that we have many such single photon sources. Such scalability, however, remains an important unsolved problem for many of these inorganic QDs due to random spatial positioning and inhomogeneous broadening. Despite several promising results on deterministic growth of these semiconductor QDs,^[71–73] there is still no large-scale demonstrations of many indistinguishable QD single photon sources. There are also very few reports on cavity integration with such deterministically positioned semiconductor QD,^[74–78] including nanohole arrays and the buried stressor growth technique,^[76–78] let alone cavity integrated array of QDs. Along with QDs, color centers have been used for solid-state single photon sources.^[79] For example, nitrogen-vacancy centers in diamond have been shown to generate high purity single photons.^[80] However, integration of diamond with large-scale visible photonics is difficult,^[81] due to the high index of diamond. As such the scalability of existing solid-state quantum emitters remains challenging even after decades of development.

Solution-processed colloidal QDs may provide a promising solution to many of these problems. QDs are already commercially successful emitters for many classical applications, including displays,^[48,82] and light-emitting diodes.^[83] While they still suffer from color impurity due to ensemble heterogeneity, and lower brightness compared with self-assembled QDs, their low-cost processing via wet chemistry (in contrast to expensive epitaxial growth or vapor deposition) and ability to integrate with most substrate has made them competitive for classical light applications. They are also leading materials for bio-imaging and microscopy.^[84] Despite their promise of scalability, their quantum properties have been viewed as poor for QISE applications. However, it is to be noted that these materials were never optimized for their quantum optical properties, and only recently have they been seriously studied for quantum light emission.^[47] Thus, in our opinion, these materials hold a lot of promise to create a scalable QISE platform.

As mentioned earlier, the experimental signature of single-photon emission is measured by the second order photon intensity autocorrelation $g^{(2)}(\tau)$,^[15] defined as:^[85]

$$g^{(2)}(\tau) = \frac{\langle \hat{a}^\dagger(t) \hat{a}^\dagger(t+\tau) \hat{a}(t+\tau) \hat{a}(t) \rangle}{\langle \hat{a}^\dagger(t) \hat{a}(t) \rangle^2} \quad (1)$$

where $a(a^\dagger)$ is the annihilation (creation) operator for photons; t denotes the time variable and τ signifies the delay between two photons. The phenomenon of $g^{(2)}(0) < 1$ signifies that the photons are anti-bunched, where as $g^{(2)}(0) > 1$ implies the pho-

tons are bunching together. In theory, for a pure single-photon state, the value of $g^{(2)}(0)$ should be equal to 0. In practice, due to background noise and imperfection of the quantum emitters, $g^{(2)}(0) < 0.5$ indicates the presence of single-photon emitters.

Single-photon emission from colloidal QDs has been measured at room temperature, providing opportunities to explore single-photon sources under ambient conditions. Brokmann et al. observed photon antibunching from a CdSe/ZnS core-shell QD with $g^{(2)}(0) < 0.05$ at room temperature^[86] (Figure 2a). Interestingly, the $g^{(2)}(0)$ value remains low even under high optical pumping power, which is attributed to an Auger process that suppresses radiative emission from the multi-exciton states. An electrically triggered single-photon source has also been demonstrated.^[87] This device consists of isolated CdSe/CdS core/shell QDs sparsely buried in an insulating layer that is sandwiched between electron-transport and hole-transport layers (Figure 2b). Under electrical pumping, single-photon emission with near-zero antibunching at room temperature was measured.

Although single-photon characteristics have been identified, to develop a high-quality single photon source based on colloidal QDs, the current challenge lies in their blinking and poor indistinguishability. Blinking, namely photoluminescence intermittency, means that there are “on” periods for the QD emission and “off” periods where the QD becomes completely dark. Several studies suggest that blinking originates from Auger recombination and surface trapping,^[88] and most research efforts focus on reducing blinking with advanced synthesis methods. Giant multi-shell CdSe QDs have been synthesized to reduce surface trap states, which efficiently suppresses blinking.^[89] Another way to reach near-complete suppression of blinking is through passivation of quantum dot surfaces, which requires adding surface binding groups or controlling the QD solution environment.^[90–92] New material systems have also been explored to address this problem. For example, InP/ZnS QDs exhibit low interfacial strain and a type I band alignment, resulting in nearly blinking-free single-photon emission with high purity^[60] (Figure 2c). Recently high purity and reduced blinking were also reported in all inorganic metal-halide perovskite (CsPbX₃) QDs.^[47,93]

Another critical drawback of solution processed colloidal QDs is they typically suffer from huge dephasing rates ($\gamma^* \approx 10^5 \times \gamma$, γ^* being the pure dephasing rate and γ being the QD dipole decay rate) at room temperature, which makes the emitted single photons highly distinguishable. Exciton-phonon interactions in these dots cause randomization of the phase of wavefunctions, which results in loss of quantum coherence and leads to dephasing, as shown by Huang et al.^[94] Apart from this, charge noise arising from fluctuations in the environment leads to small DC shifts in the emitter transition energy contributing to further decoherence.^[95] With both effects combined, the indistinguishability of colloidal QDs is limited. For typical quantum emitters with a large dephasing rate, the indistinguishability I of emitted photons is given by^[96,97]

$$I = \frac{\gamma}{\gamma + \gamma^*} \quad (2)$$

where, γ is the radiative decay rate and γ^* is the pure dephasing rate of the quantum emitter. Hence for colloidal QDs, where

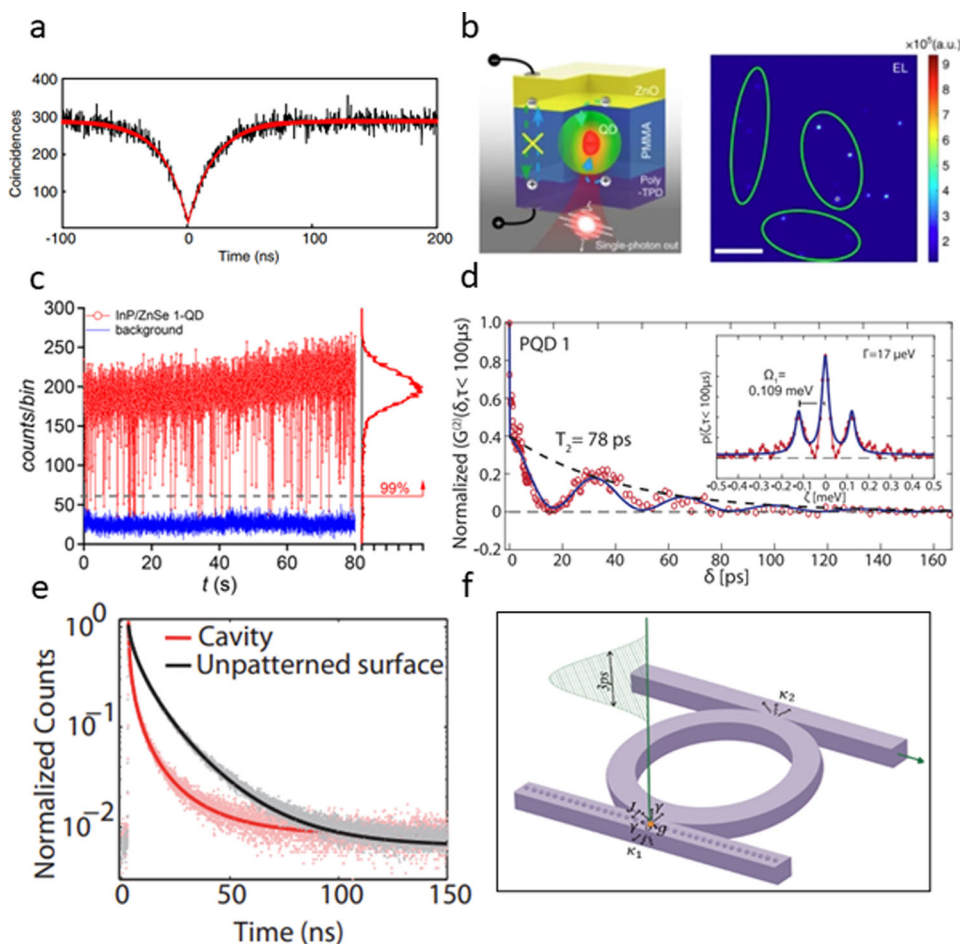


Figure 2. Single-photon source based on colloidal QDs. a) Single-photon emission from a CdSe/CdS core-shell quantum dot^[86] (antibunching with $g^2(0) < 0.05$). b) Electrically triggered colloidal single-photon source.^[87] The device consists of isolated CdSe/CdS core/shell quantum dots sparsely buried in an insulating layer that is sandwiched between electron-transport and hole-transport layers. c) InP/ZnS QDs shows nearly blinking-free single-photon emission with high purity.^[60] d) Coherent single-photon emission from colloidal lead halide perovskite quantum dots.^[47] e) Purcell enhancement of CdSe colloidal QDs coupled to nanobeam cavity.^[98] f) Improving indistinguishability of the emitted single photons by heterogeneous photonic molecule.^[102] Figures are reprinted with permission: a) Reproduced with permission.^[86] Copyright 2004, IOP Publishing. b) Reproduced with permission.^[87] Copyright 2017, Macmillan Publishers Ltd. c) Reproduced with permission.^[60] Copyright 2017, American Chemical Society. d) Reproduced with permission.^[47] Copyright 2019, AAAS. e) Reproduced with permission.^[98] Copyright 2013, Optical Society of America. f) Reproduced with permission.^[102] Copyright 2019, American Chemical Society.

$\gamma^* \approx 10^5 \gamma$ the indistinguishability I turns out to be $\approx 10^{-5}$, making it impossible to use the bare emitter as a useful indistinguishable single-photon source.

Further improvement of indistinguishability of emitted single photons is expected from progress in synthesis techniques and new materials like perovskite QDs. Recently, all inorganic metal-halide perovskite QDs with optical coherence times (T_2) of up to 80 ps were demonstrated^[47] (Figure 2d). With a radiative lifetime (T_1) of 210 ps, the bare emitter indistinguishability I from these perovskite QDs approaches $I \approx \frac{T_2}{2T_1} \approx 0.19$. This is a two to three orders of magnitude improvement from the standard colloidal QDs, which fundamentally suffer from slow photon release from dark exciton states. These results could pave the way for the future development of indistinguishable solution-processed quantum emitters that have fast emission, wide spectral tunability, and scalable production.

Besides progress in material synthesis to develop a bright single-photon source with high indistinguishability, integration with nanophotonic cavities may prove to be indispensable. Coupling a single-photon emitter with a high-quality factor and small mode volume photonic cavity could enhance the spontaneous emission rate via Purcell enhancement.^[85] The enhanced spontaneous emission rate would then lead to brighter emission and higher indistinguishability (larger than $\frac{T_2}{2T_1}$). Gupta et al. demonstrated Purcell enhancement and saturable absorption in CdSe/CdS QDs coupled with a SiN photonic crystal.^[98] An average Purcell enhancement of 4.6 was observed (Figure 2e), together with a narrowing of the linewidth with increasing pump intensity due to saturable absorption. Similar experiments on perovskite QDs coupled with photonic crystal cavities have also been demonstrated.^[99,100] The Purcell enhancement factor for such emitter-cavity systems is given by:

$$F_{\max} = 1 + \frac{3\lambda^3}{4\pi^2 n^2} \frac{Q_{\text{em}}}{V} \psi(r) \quad (3)$$

Here, λ is the cavity resonance wavelength; Q_{em} is the Q-factor of the emitter linewidth; n is the refractive index of the cavity dielectric; V is the cavity mode volume; and $\psi(r)$ is the ratio of the mode intensity at the emitter's location to the maximum. We note that we are using the Q-factor of the emitter but not the cavity since we are in the "bad" emitter regime, where the linewidth of the emitter is much larger than that of the cavity. This is in contrast to the self-assembled QDs or color centers, where the system is in the "good" emitter regime, that is, the emitter linewidth is narrower than the cavity linewidth, the Q_{em} is replaced by the Quality factor of the cavity in the above equation.^[101]

Saxena et al. proposed a system consisting of two coupled optical cavities, one of which is coupled to a single colloidal QD.^[102] The device is designed in a manner such that the cavity containing the colloidal QD has a small mode volume and a moderate quality factor and is weakly coupled to another cavity with an extremely high quality factor (Figure 2f). In such a configuration adiabatic elimination of coherence in optical Bloch equations shows that the first cavity acts as an effective emitter for the second cavity, which funnels this collective emission into its narrow linewidth. The emitted photons from this second cavity are expected to have very high indistinguishability ($I \approx 0.9$). The predicted indistinguishability of these photons is on par with other commonly used dissipative quantum emitters like silicon-vacancy centers^[103] and self-assembled QDs.^[97]

2.1.1. Outstanding Challenges

Experimentally, indistinguishability could be measured via HOM interference.^[104] Indistinguishability is manifested by the HOM interference visibility (V), and a perfect indistinguishability yields $V = 1$. For self-assembled QDs, indistinguishability values well above 90% have been experimentally measured.^[105,106] To the best of our knowledge, such measurements have not yet been reported for colloidal QDs, and the non-transform limited spectrum of these QDs already indicates low indistinguishability. This will be an important milestone to achieve in the field of solution-processed quantum emitters.

Besides single photons, QDs can also generate entangled photons through the biexciton–exciton (XX–X) radiative cascade.^[107,108] As mentioned above, spontaneous parametric down-conversion, the most widely used process for generating entangled photons, has an inherent limitation in terms of efficiency. Recently, an entangled photon pair source with record-high brightness and indistinguishability generated by self-assembled GaAs QDs has been demonstrated.^[109] While the generation of entangled photons has not yet been demonstrated in a colloidal QD platform, it would be an important future research direction.

Another intriguing research direction is to extend the emission wavelength to the near IR wavelength region,^[110] where it is compatible with silicon photonics and the optical fiber network. Foell et al. observed saturable photoluminescence of PbSe QDs coupled with silicon photonic crystals at ≈ 1550 nm. The saturation was attributed to a non-radiative exciton decay channel

by fitting the experiment with a quantum optics model.^[111] IR-emitting PbS QDs also have been integrated with photonic crystal cavities, but no single photon emission has been reported.^[110] Hence further research efforts are required to isolate single QDs and verify single-photon emission from near-IR-emitting QDs.

2.2. Deterministic Positioning on Nanophotonic Structures

As mentioned earlier, one outstanding challenge of coupling self-assembled QDs and color centers to photonic cavities has been the random positioning of these emitters. There are several reports on deterministic growth of QDs or implantation of color centers but aligning the cavities with these emitters is challenging.^[76–78,112] As such, a scalable approach to couple deterministically grown emitters to cavities has not been demonstrated. This is where solution processed emitters could be beneficial. In fact, several recent works reported deterministic positioning of colloidal QDs on nano-cavities. Chen et al. demonstrated a deterministic positioning mechanism based on lithographically-defined masking^[113] (Figure 3a). By lithographically defining a window on top of a nanobeam cavity that is encapsulated by a polymer resist,^[51] and spin coating the QD solution, the placement of QDs could be precisely controlled. Further improvement of the fabrication process could potentially push the number of deterministically positioned QDs down to a single-dot level.^[114] For example, by making the windows smaller (≈ 50 nm) and synthesizing giant QDs (≈ 50 nm diameter),^[89] the number of QDs landing inside the windows could be effectively reduced. Recently, deterministic positioning of a single colloidal QD on an integrated photonics waveguide has also been demonstrated^[115] (Figure 3b). The fabrication processes are similar to the work by Chen et al., with an additional lift-off process to clean the residual QDs landing outside the targeted sites. This lift-off process allows for iterative polymer resist patterning, which provides a viable method to position single emitters at predefined positions in a photonic integrated circuit with a high yield.^[115] As shown in Figure 3, the red circles mark sites that show photon statistics consistent with single-photon emitter occupancy (12 out of 20), after two iterative patterning-deposition-lift-off processes. Moving forward, more advanced deposition methods such as Langmuir–Blodgett deposition^[116] could be applied to precisely control the layer number and the uniformity of a QD thin film, leading to a higher yield and better reproducibility. Novel nanophotonic design could also improve control over the coupling to QDs. For example, a nano-pocket design inside the nanobeam cavity has been recently demonstrated^[117] (Figure 3d), where a low mode volume and high coupling efficiency are simultaneously achieved. Together with various active tuning mechanisms of the integrated photonic devices,^[57,118] deterministically-positioned colloidal QD systems show potential to create a scalable cavity quantum electrodynamic platform. Another outstanding challenge will be to circumvent the inhomogeneous broadening of the solution-processed QDs, which will require in situ tuning of the QD resonance frequency. Several reports exist of Stark tuning of the colloidal emitters,^[119–122] which can be employed to mitigate the inhomogeneous broadening. Additionally, better synthesis techniques to reduce the inhomogeneous broadening need to be explored to ensure the desired scalability.

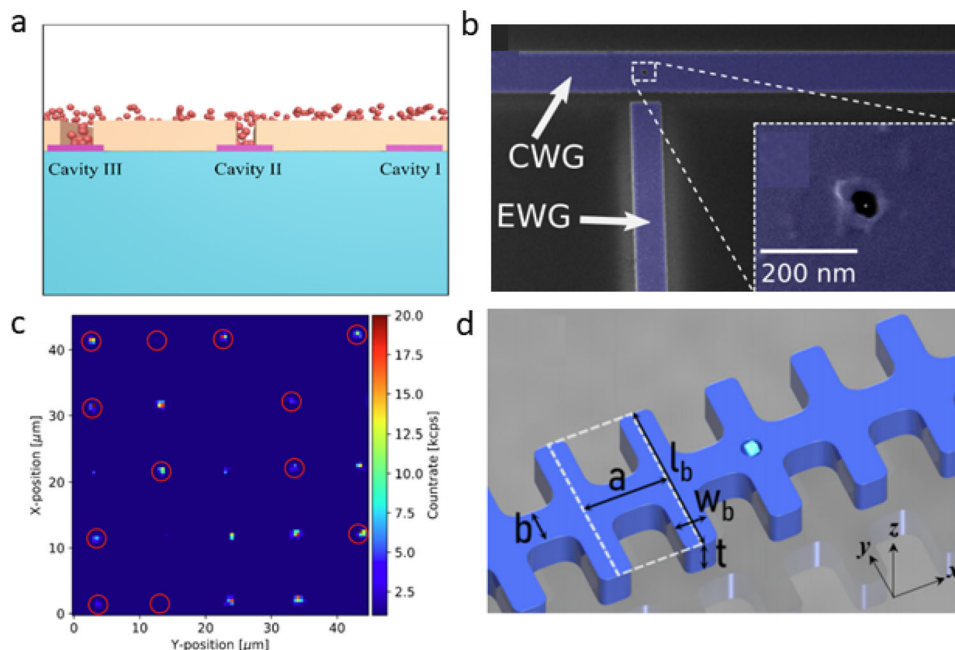


Figure 3. Deterministic QD positioning on nanophotonic structures. a) Deterministic positioning of QDs on a silicon nitride nanobeam.^[113] b) A single QD deterministically positioned in a tantalum pentoxide waveguide.^[115] c) The lift-off process allows the iterative polymer resist patterning,^[115] which provides a viable method to position single emitters at predefined positions in a photonic integrated circuit with a yield that approaches unity. d) A nano-pocket design inside the nanobeam cavity allows both low mode volume and high coupling efficiency.^[117] Figures are reprinted with permission: a) Reproduced with permission.^[113] Copyright 2018, American Chemical Society. b,c) Reproduced with permission.^[115] Copyright 2021, The Authors. d) Reproduced with permission.^[117] Copyright 2020, American Chemical Society.

2.3. Nano-Laser

As explained earlier, the indistinguishability of single-photon sources is of utmost importance for quantum applications. While dephasing of solution processed QDs primarily comes from charge fluctuations and phonons, through improved synthesis and moving to lower temperatures these dephasing times can be significantly reduced. However, there will still be residual dephasing from carrier relaxation associated with higher-order excited states. In fact, this is currently the primary source of dephasing and distinguishability for self-assembled QDs.^[123,124] One way to get rid of this additional dephasing is via resonant excitation.^[123,125] However, this requires large external lasers, which preclude scalability. One promising solution is to create on-chip lasers. These lasers do not need to have high power, and thus nano-scale lasers may be an ideal solution.^[126–128] Thus, while lasers still emit classical coherent light, they could be an important tool in quantum photonics. Given the long history of nano-lasers using solution-processed materials, it is important to review the progress in this area for quantum nanophotonics.

The two critical components of a laser are the gain medium and the optical cavity. For colloidal QDs the optical gain mechanism has been thoroughly discussed.^[129–132] Here we focus on various nanophotonic structures to achieve lasing in a colloidal QD platform. Most colloidal nanolasers, such as, perovskite-based lasers, have relied on the self-assembly of the solution-processed material,^[133–136] where the solution-processed material serves both as the gain medium and the optical cavity, including whisper gallery mode resonators and nanowire cavities.^[133–136]

While this intrinsic cavity structure has the advantage of low-cost synthesis, the lasers always exhibit a broad linewidth that is not suitable for most applications, and the self-assembly process introduces disorder and randomness, precluding fabrication of an array of lasers with identical structures.

Continuous efforts have been devoted to integrating colloidal QDs with high-quality cavities that emit light into a well-defined spatially and temporally coherent mode.^[137–139] By coupling the solution-processed material to an integrated nanophotonic cavity, the spontaneous emission coupling factor, also known as the β factor could be enhanced via the Purcell effect, resulting in a reduction of the lasing threshold.^[140] The β factor is defined as

$$\beta = \frac{\Gamma_{\text{cav}}}{\Gamma_{\text{cav}} + \Gamma_{\text{other}} + \Gamma_{\text{nr}}} \quad (4)$$

Here, Γ_{cav} is the radiative decay rate into the cavity mode, Γ_{other} is the decay rate into other optical modes, and Γ_{nr} is the nonradiative decay rate. Purcell enhancement could increase Γ_{cav} , resulting in a higher β factor. With more radiative coupling channeled into the laser modes, the lasing threshold would subsequently be reduced.

Table 1 summarizes the performance of existing integrated lasers based on solution-processed materials. Xie et al. demonstrated a silicon nitride microdisk laser integrated with CdSe QDs, with a threshold of $27 \mu\text{J cm}^{-2}$ with a picosecond pumping pulse.^[137] The microdisk consists of a SiN/QD/SiN sandwich that supports high-Q whispering gallery modes with a maximum optical field in the central QD layer (Figure 4a). A silicon

Table 1. Performance of existing integrated lasers based on solution-processed material.

| Material | Cavity structure | Lasing wavelength | Threshold | Pumping source |
|------------------------------|-----------------------------|-------------------|----------------------------|-------------------|
| CdSe/CdS QD ^[137] | SiN microdisk | 630 nm | 27 $\mu\text{J cm}^{-2}$ | Picosecond laser |
| CdSe/CdSQD ^[141] | SiN DFB | 630 nm | 270 $\mu\text{J cm}^{-2}$ | Nanosecond laser |
| Perovskite ^[142] | SiN nanobeam | 688 nm | 5.62 $\mu\text{J cm}^{-2}$ | Picosecond laser |
| Perovskite ^[143] | Perovskite microdisk on SiN | 785 nm | 4.7 $\mu\text{J cm}^{-2}$ | Femtosecond laser |
| CdSe/CdS QW ^[99] | SiN nanobeam | 658nm | 0.97 μW | CW laser |

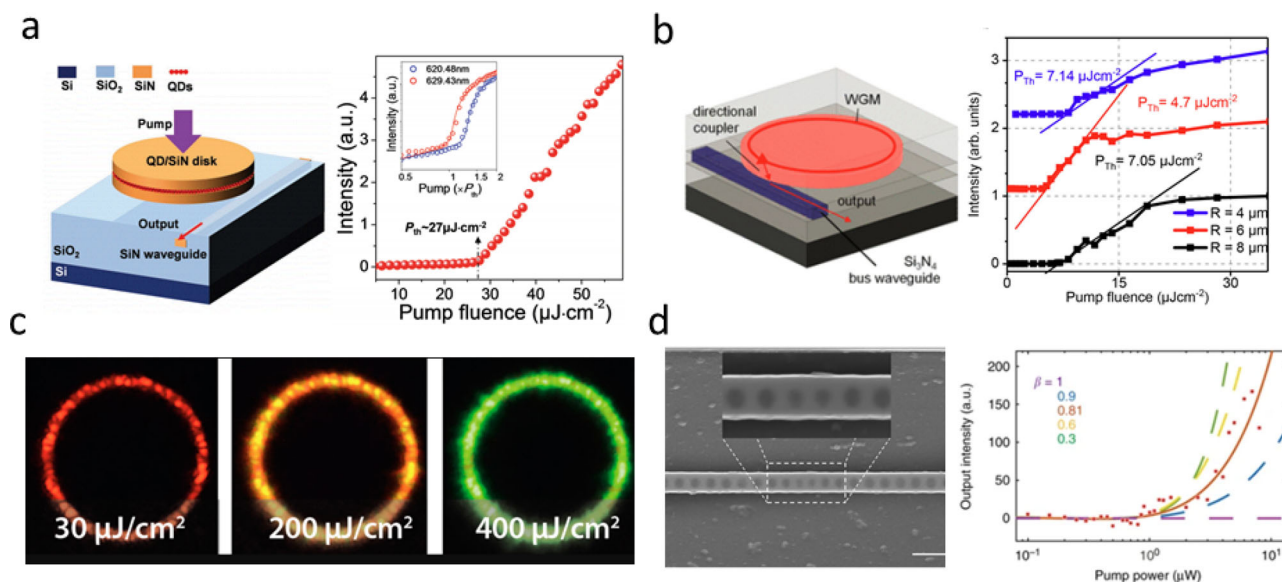


Figure 4. Integrated lasers based on solution-processed material. a) The microdisk laser consists of a SiN/QD/SiN sandwich that supports high-Q whispering gallery modes with a maximum of optical confinement in the central QD layer.^[137] b) Perovskite laser monolithically integrated on a silicon nitride platform.^[143] c) Active laser color control in a core-shell CdSe/CdS QD ring laser fabricated by the template-stripping method.^[138] d) A CW laser achieved by coupling colloidal QWs to a silicon nitride nanobeam cavity.^[148] Figure are reprinted with permission: a) Reproduced with permission.^[137] Copyright 2017, Wiley-VCH. b) Reproduced with permission.^[143] Copyright 2018, American Chemical Society. c) Reproduced with permission.^[138] Copyright 2018, American Chemical Society. d) Reproduced with permission.^[148] Copyright 2017, Macmillan Publishers Ltd.

nitride distributed feedback (DFB) laser with a similar sandwich structure has also been demonstrated,^[141] with a threshold of 270 $\mu\text{J cm}^{-2}$ under nanosecond pulse pumping. Recently, perovskite nanocrystals have emerged as another novel light-emitting material with excellent gain properties. Lasing from perovskite QDs coupled to a silicon nitride nanobeam platform has been demonstrated, with a lower lasing threshold of 5.62 $\mu\text{J cm}^{-2}$ under picosecond pulse pumping.^[142] Cegielski et al. monolithically integrated methylammonium lead iodide perovskite microdisk lasers into silicon nitride integrated photonics platform^[143] (Figure 4b). The laser exhibits a low threshold of 4.7 $\mu\text{J cm}^{-2}$ under femtosecond pulse pumping.

Improvements in cavity fabrication have also triggered the exploration of other novel lasing phenomena, such as, color switching. Feber et al. demonstrated active laser color control in a core-shell CdSe/CdS QD ring laser,^[138] which is fabricated by a template-stripping method. As pumping power increases, the gain medium pivots from the CdSe core to the CdS shell, resulting in a laser color switch from red to green (Figure 4c). This color-switch behavior is explained by a rate-equation model as a

competition between exciton localization into the core and stimulated emission from excitons in the shell.

Despite recent developments in cavity fabrication, so far, most nanophotonic colloidal QD lasers still work under pulsed optical pumping. A successful demonstration of continuous-wave (CW) pumping would be a breakthrough, and an important step toward an electrically pumped laser, which will provide a true integrated solution. The main challenge, however, lies in Auger recombination, a non-radiative emission channel with a decay rate proportional to the cube of carrier density. Studies show that the Auger process is much more efficient in nanometer-sized emitters.^[86] For colloidal QDs, the Auger recombination rate is on the picosecond time scale, which is much faster than the bimolecular radiative recombination rate (nanosecond time scale). Continuous efforts have been devoted to suppressing Auger recombination to lower the lasing threshold. Recently, advanced facet-selective epitaxy synthesis of colloidal QD solids shows promising results and achieves continuous-wave lasing.^[144] Yet the integration of such colloidal QD solids with nanophotonic cavities remain challenging.

To achieve CW lasing in a solution-processed material platform, colloidal quantum wells (QWs) or nano-platelets (NPL) provide a promising solution thanks to their suppressed Auger recombination and narrower emission linewidths compared to traditional 0D QDs.^[145] She et al. demonstrated amplified spontaneous emission (ASE) from colloidal QW with a threshold as low as $6 \mu\text{J cm}^{-2}$ and a gain as high as 600 cm^{-1} ,^[146] which are both significant improvements over colloidal QDs. A CW biexciton laser at room temperature was first demonstrated by Grim et al.,^[147] where the colloidal QWs were sandwiched by a pair of DBR mirrors. To further reduce the lasing threshold, by coupling the QW with a silicon nitride nanobeam cavity, Yang et al. demonstrated a CW laser with a low-threshold less than $1 \mu\text{W}$ ^[148] (Figure 4d). One interesting research direction will be to explore new physics, like parity-time-symmetric and non-Hermitian physics, on the laser platform. Efficient gain from solution-processed materials offers a great opportunity to manipulate the gain and loss in coupled optical cavity systems.^[149,150]

Despite recent progress of optically pumped lasers, the goal to demonstrate electrically pumped lasing remains challenging in solution-processed material platforms due to the limited charge transport properties from insulating ligands. We would like to point out that electrically pumped nano-lasers providing short pulses are much more integrable and scalable for the on-demand generation of single photons. Recently, electrically controlled ASE in colloidal QDs has been demonstrated.^[151] The device consists of a colloidal QD film that is sandwiched between two dielectric layers, forming a capacitor to apply an electrical field. A 10% reduction in the ASE threshold is observed in a 264 kV cm^{-1} electrical field. Combined with kinetic equation modeling, the experimental results indicated that 17% of the colloidal QD population is charged. Further analysis suggested that if the entire colloidal QD population is charged, a 35% lowering of the ASE threshold could be achieved. This work showed that good control of the charging process for the colloidal QD film will significantly improve colloidal QD lasers and lower the ASE threshold, with potential to achieve electrically driven nano-lasers. Along with the ASE studies of electrically driven colloidal QD thin films, novel designs to incorporate an optical cavity structure into the current colloidal LED configuration are also important. Roh et al. developed a structure where a DFB resonator is integrated into a bottom LED electrode.^[152] This device exhibited strong electroluminescence under electrical pumping and low threshold lasing under optical pumping. This practical architecture paves the way toward colloidal QD lasing with electrical injection.

3. Strong Light-Matter Interactions

The previously reported effects, including non-classical light generation and single photon sources, primarily operate in the weak coupling regime, that is, the coherent light-matter interaction strength between the exciton and cavity mode is smaller than the system losses (cavity loss and exciton decay rate). In this regime, the enhancement due to the cavity is well described by the Purcell effect, which provides a perturbative treatment of the exciton-cavity interaction. When the coherent interaction strength surpasses the system loss rates, then the photon and exciton hybridize to create a new type of quasi-particle called an exciton-polariton (EP).^[153] In this regime, the simple pertur-

bative treatment is no longer valid, and full quantum optical modeling is required. EP provides a promising platform to achieve strong interactions between two single photons, namely, quantum nonlinear interactions,^[154] which are required for non-trivial two-qubit quantum gates^[35] and photonic quantum simulation.^[155] Quantum nonlinearity has been demonstrated on self-assembled QDs strongly coupled to a photonic crystal platform,^[36] and recently some progress has also been made on an epitaxially-grown QW-coupled micro-cavity platform.^[156] In the meantime, condensates in EP systems have been long studied as “quantum fluids of light” for quantum simulation.^[155,157–159] Similar ideas could potentially be transferred to a colloidal-based EP system, with the advantage of low-cost material synthesis and potential room-temperature operation.^[160,161]

3.1. Exciton Polariton

EPs inherit a low effective mass from their photonic component and large nonlinear interaction strength from their excitonic component, making them a promising platform to study many-body quantum effects, including Bose–Einstein condensates,^[159] and EP-mediated superconductivity,^[162] with far-reaching impact on quantum simulation with interacting photons. The current field of EPs is predominantly based on epitaxial InAs-GaAs QW excitons coupled to a DBR cavity. These cavities are grown via the same epitaxy process used to grow the QW. Several seminal experiments have demonstrated polariton condensates, polaritonic lasing and nonlinear optical switching in these III–V inorganic QW systems.^[159,163,164] However, these QW materials require epitaxial growth, making the process expensive. Additionally, they are not compatible with large-scale silicon/silicon nitride manufacturing processes. Finally, most of the reported experiments involve out-of-plane diffuse Bragg reflector (DBR) cavities, which are not conducive to integrated photonic applications. By guiding light in-plane, a scalable photonic circuit can be created as needed for quantum photonics.

To study the EPs with solution-processed materials, the relatively broad linewidth of the colloidal QDs remains a challenge, though recently strong coupling of a single QD to a Fabry–Perot (F-P) cavity of the dielectric SiO_2/Si material has been reported.^[165] As explained earlier, solution-processed QWs or NPLs, on the other hand, can provide an excellent platform to probe EPs, due to their small inhomogeneous broadening, and strong exciton binding energy. Flatten et al. demonstrated strong coupling of colloidal QWs with a micrometer-scale Fabry–Perot cavity^[166] (Figure 5a). Vacuum Rabi splittings of $66 \pm 1 \text{ meV}$ and $58 \pm 1 \text{ meV}$ were reported for the heavy and light hole excitons, respectively.

One popular research direction in the EP community is to reach the Bose–Einstein condensation (BEC) regime, where many polaritons condense into the lowest quantum state in the system. The condensation starts with a large number of polaritons injected into the system, which are then scattered by phonons to lower energy states called the “bottleneck” region in the polariton dispersion diagram.^[157] For the polaritons inside the “bottleneck” region, the polariton–polariton interaction plays a critical role in scattering them into further lower energy states around zero momentum. As the density of the polaritons around

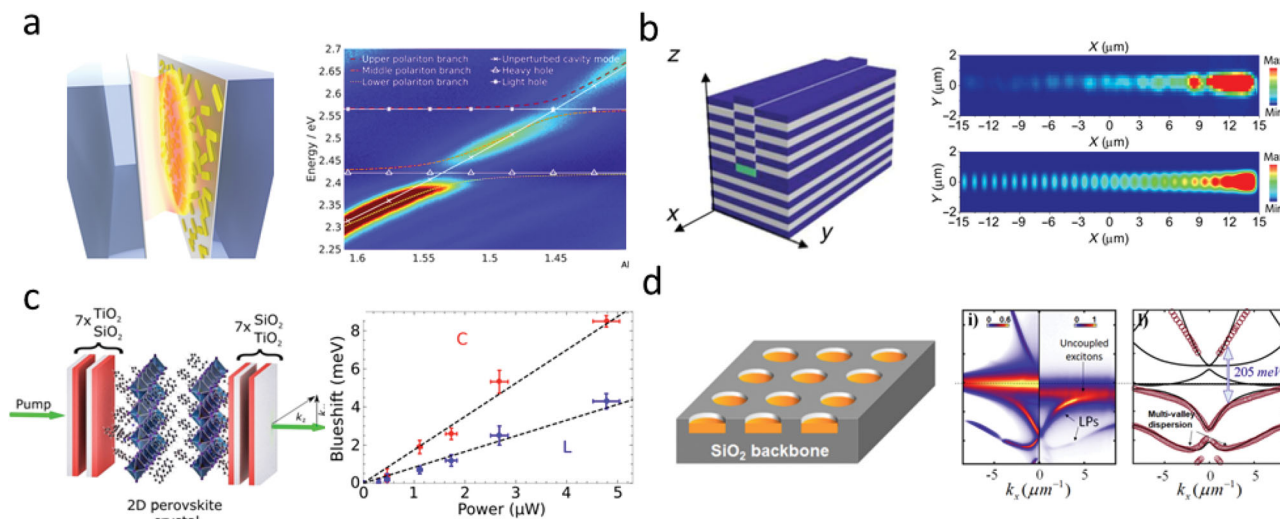


Figure 5. Exciton polaritons. a) Strong coupling of colloidal QWs with micrometer-scale Fabry–Perot cavity.^[166] b) Room temperature long-range coherent exciton-polariton condensate flow in lead halide perovskites.^[160] c) Polariton–polariton interaction at room temperature of perovskite in an FP cavity, manifested by the blueshift of the lower polariton.^[177] d) Strong coupling between a perovskite and a metasurface with a Rabi splitting: Various shapes of polariton dispersion.^[54] Figures are reprinted with permissions: a) Reproduced with permission.^[166] Copyright 2016, American Chemical Society. b) Reproduced with permission.^[160] Copyright 2018, AAAS. c) Reproduced with permission.^[177] Copyright 2019, AAAS. d) Reproduced with permission.^[54] Copyright 2020, American Chemical Society.

zero momentum increases, above a certain threshold, condensation occurs.^[159] In this regime, all the polaritons follow Bose–Einstein statistics and condense into the lowest energy state in the system. The signature of BEC is probed by measuring the cavity-emitted photons: above the threshold, the emission spectrum goes through a narrowing of the linewidth and exhibits a kink in the emission intensity. During this process, coherent photon emission, namely, polariton lasing, is generated without the need for population inversion. As a result, the polariton laser possesses a lower threshold compared to photon laser and has been extensively studied on the InAs–GaAs QW systems.^[167] Recently, on a colloidal-based EP platform, room temperature all-inorganic perovskite QW polariton lasing has been demonstrated.^[168] The platform is based on an epitaxy-free all-inorganic CsPbCl₃ perovskite nanoplatelet embedded in a DBR-based Fabry–Perot cavity. Polariton lasing on this platform is confirmed by a super-linear power dependence, macroscopic ground-state occupation, a blueshift of the ground-state emission, narrowing of the line width, and a buildup of long-range spatial coherence.^[168] These results pave the way for future development of ultra-low threshold room-temperature polariton lasers.

Along with low-threshold coherent emission, polaritonic BEC also provides a unique platform to study superfluidity,^[169,170] solitons,^[171,172] and quantum phase transitions.^[173] The photonic part of the system allows the use of an optical microscope to probe these fascinating physics.^[174] For example, the most compelling evidence of superfluidity so far is the measurement of Rayleigh scattering from a polariton condensate in the presence of an obstacle.^[169,175] Experimentally, polariton flow could be excited by a laser beam, and the polariton density could be well-controlled by the optical power of the laser. At low density, when the polariton flow comes across an obstacle during its propagation, the polaritons would be elastically scattered due to the parabolic dispersion of the lower polariton branch.

When the BEC is reached at high density, however, the parabolic dispersion is perturbed into the Bogoliubov dispersion by the strong polariton–polariton interaction.^[157,176] Under the Bogoliubov dispersion regime, when a condensate flowing with a velocity smaller than the Landau velocity hits the obstacle, there are no resonant states to scatter into. As a result, the moving condensate shows the emergence of friction-less flow in the superfluid regime. The above phenomenon has been well observed in epitaxially-grown InAs–GaAs QW systems.^[169] Recently, polariton flow and polariton–polariton interaction in colloidal-based EP systems have been reported. Su et al. demonstrated room temperature long-range coherent exciton-polariton condensate flow in lead halide perovskites coupled to a DBR cavity^[160] (Figure 5b). The perovskite polariton condensate exhibits high-speed propagation over macroscopic distances of 60 μm while still preserving the long-range off-diagonal order at room temperature. Fieramosca et al. studied the polariton–polariton interaction of 2D organic-inorganic perovskites coupled to a DBR cavity at room temperature (Figure 5c). A polariton–polariton interaction strength of $\approx 3 \pm 0.5 \mu\text{eV} \mu\text{m}^2$ was experimentally extracted.^[177] This value is two orders of magnitude higher than the values measured for organic excitons,^[170] and is the largest polariton–polariton interaction strength measured at room temperature. Wu et al. experimentally demonstrated nonlinear parametric scattering of perovskite EPs at room temperature,^[178] driven by the scattering source from condensation in one polariton branch, an energy-degenerate parametric scattering signal was obtained in high momentum states in an adjacent branch. Such nonlinear parametric scattering has been previously observed in a GaAs polaritonic system at cryogenic temperature.^[179] All the aforementioned EPs were observed in a Fabry–Perot resonators with the mirrors being DBR stacks. Overall, the observation of condensate flow and strong nonlinearity at room temperature shows the promise of future polariton devices based on solution-processed

materials. In the meantime, these demonstrations pave the road for future study of fascinating physics including superfluidity and solitons in colloidal-based EP platforms.

Along with DBR-based Fabry–Perot cavities, other nanophotonic cavities have been used to study EPs, including nanowire cavities and guided-mode resonators. A nanowire cavity could be synthesized by low-cost wet chemistry.^[180] The strong confinement of the optical mode in the nanowire, together with the large spatial overlap with the excitons in the material, result in a larger light-matter interaction strength compared to the regular DBR-based Fabry–Perot cavity. The photons are coupled out from the nanowire toward the in-plane direction, which favors the integration with quantum photonic circuits. Zhang et al. demonstrated the strong exciton-photon coupling in a perovskite nanowire cavity, with a vacuum Rabi splitting energy up to 390 meV.^[181] Besides strong light-matter coupling, Zhu et al. also demonstrated continuous wavelength lasing of perovskite nanowires from polariton modes.^[182] Guided-mode resonators provide another promising platform to realize compact polaritonic devices. This type of resonator was first studied by Fan et al. in photonic crystal structures.^[183] The periodic 2D photonic lattice supports many optical Bloch modes propagating inside the slab. These modes can be classified into two classes, namely, in-plane guided modes and guided-mode resonance. These guided mode resonators couple with the radiation continuum and confine part of their electromagnetic energy inside the slab. When a light beam shines on the photonic lattice, interference between the slab mode and the guided modes results in a Fano line shape in the reflection spectrum. These Fano resonances have various angle-dependent dispersive spectra, and when strongly coupled with excitons, an anti-crossing is expected to occur around the exciton wavelength. Fujita et al. showed strong coupling between a perovskite and a 1D guided mode resonator at room temperature^[184] and a Rabi splitting value of 100 meV was extracted. Recently, this platform was extended to a 2D guided mode resonator, also called a non-local metasurface.^[185] Dang et al. demonstrated strong coupling between the metasurface and the exciton resonance with a Rabi splitting in the 200 meV range.^[54] Moreover, various shapes of polariton dispersion, including parabolic, linear, and multivalley, have been observed by advanced meta-optical engineering (Figure 5d). The ability to sculpt the polaritonic dispersion and polariton lifetime in such platforms provides extra opportunities to study exotic physics in the EP system, including ballistic propagation of polariton and momentum-space Josephson effects.^[54] A recent demonstration of topological polaritons in a 2D metasurface platform also provides the opportunity to merge topological physics together with EP in the future.^[186,187] As such, novel nanophotonic structures, including bound states in continuum^[188] and other kind of meta-optical structures^[189] could provide novel functionalities for quantum technologies based on solution processed materials.

3.2. Polaritonic Lattice

Moving forward, the ability to manipulate the complex energy potential landscape in EP systems is required for EP-based quantum simulators.^[190] The idea of quantum simulation as proposed by Feynman is to simulate a complex quantum system with an-

other quantum system that is more readily controlled. A critical need for such quantum simulation is to create a lattice of quantum nodes.^[191] The interplay of nonlinear interaction between light at each node and coherent coupling between each node is at the heart of many quantum simulation methods.

The above configuration could be realized by patterning a DBR-based FP cavity into an array of coupled micropillars with on-site excitonic nonlinearity.^[190] Due to the ease with which various design geometries that have been made possible through advances in micro- and nano-fabrication, such a platform is an ideal candidate for simulating various condensed matter physics including pivotal spin Hamiltonians.^[192] Engineering the underlying device lattice allows control over the coupling between the spin and momentum degrees of freedom of the polaritons and the strong non-linearities involved allow for observing signatures arising from the interplay of on-site interactions and spin-orbit effects.^[193] Also, leveraging the on-site nonlinearity, a coupled EP system based on two micropillars could already simulate several fascinating physical phenomena,^[194] such as, the nonlinear bosonic Josephson junction, whose dynamics are intimately related to the Josephson effect in superconductors. Abbarchi et al. experimentally observed the nonlinear Josephson oscillation of two coupled polariton condensates confined in a photonic molecule.^[194] At low densities, the coherent oscillations of particles tunneling between the two sites are observed. At high densities, interactions quench the transfer of particles, inducing the macroscopic self-trapping of polaritons in one of the micropillars. Further increasing the number of coupled cavities would result in the formation of a band-structure in the polariton lattice. Among various band structures existing in the solid-state system, the flat-band dispersion is of great interest. Flat bands have been shown to be related to spin liquids,^[195] the fractional quantum hall effect,^[196] and superconductivity.^[197] In the flat band, the system has zero velocity with infinite mass. As a result, the density of states increases and the system becomes extremely sensitive to interaction and perturbation.^[198] Also, the very large mass significantly alters the effects of disorder on flat band systems with the possibility of existence of inverse Anderson delocalization transitions deviating from the standard observed Anderson localization phenomena.^[199] On the coupled-cavity platform, the flat band could form in a 1D Lieb lattice. Goblot et al. demonstrated the flat-band experimentally based on the coupled InGaAs/GaAs micropillars,^[200] where the EPs with bright quantized nonlinear domains and sharp edges were observed. Combined with theoretical modeling, these nonlinear domains are shown to be part of the family of gap solitons named truncated Bloch waves,^[201,202] which had never been observed in a driven-dissipative system previously.

Similar ideas could be transferred to the colloidal-based EP system, with the advantage of low-cost material synthesis and potential room-temperature operation. Recently, Su et al. showed perovskite polariton lattice condensation at room temperature.^[161] The initial structure consists of a poly(methyl methacrylate) (PMMA) layer on top of a perovskite layer, both embedded in a DBR-based FP cavity. The micropillar lattice is then created by patterning a PMMA layer with electron-beam lithography. A large bandgap with a value of 13.3 meV is formed in the lattice, which is at least 10 times larger than previously reported systems.^[203–205] Such a large bandgap prevents interband

transitions due to external perturbations and therefore provides robust confinement of polaritons within the lattice sites. Above a critical density, polariton condensation with long-range spatial coherence is observed at room temperature. The polariton lattice has also been demonstrated in an organic solution-processed material platform.^[206] Here the coupled cavities are formed by sandwiching the organic molecule layer by a planar DBR mirror and an array of concave mirrors made by ion milling. Bosonic condensation is observed, together with a localized gap state which is identified by real-space expansion of the condensate. The recent development of polariton lattice based on the solution-processed material platform, along with the observation of condensation at room temperature, opens a route to the implementation of polariton condensate-based quantum simulators at room temperature.

3.3. Single-Photon Nonlinear Optics

A critical requirement for any photonic quantum simulation is strong nonlinear interaction between photons. A solid-state-based quantum simulator for the Fermi-Hubbard model, if realized, would be a significant breakthrough for simulating outstanding problems in condensed matter physics, such as, high-temperature superconductivity and fractional quantum Hall physics.^[99] Coupled photonic cavities with on-site single-photon nonlinearity have the potential to simulate the Fermi-Hubbard model.^[100,101] To build such a platform, strong photon nonlinearity at the single-photon level is needed. Such nonlinearity in terms of photon blockade has been demonstrated in self-assemble QDs strongly coupled to an optical cavity.^[102–104] Recently, epitaxial QW-based cavity polaritons also show signatures of quantum anharmonicity resulting from polariton–polariton interaction in the system.^[105,106] This work shows that even without strong 3D quantum confinement of excitons, strong photon-photon interactions can be realized just by engineering the spatial confinement of photonic wave-functions. Here we review the progress on evaluating the interaction strength on the colloidal QW-based polariton platform.

For a QW coupled with a low mode-volume 0D optical cavity under a frame co-rotating with the external pump laser and setting $\hbar = 1$, the dynamics are described the Hamiltonian

$$H = \Delta\omega_x b^\dagger b + \Delta\omega_c a^\dagger a + g (a^\dagger b + b^\dagger a) + Ub^\dagger b^\dagger bb + E (a^\dagger + a^\dagger) \quad (5)$$

where b (b^\dagger) and a (a^\dagger) are the annihilation (creation) operators for the exciton and cavity modes respectively, $\Delta\omega_x$ and $\Delta\omega_c$ are the detunings of the exciton and cavity mode resonances from the pump laser frequency, respectively; g is the exciton-cavity coupling strength; U is a Kerr-type nonlinearity representing the exciton–exciton interaction strength, and E is the strength of the pump laser. We note that a 0D cavity, such as a nanobeam resonator, can support only a certain number of k -vectors, which will be coupled to the 2D exciton. Hence, we can model this system without keeping track of all the excitonic in-plane k -vectors.^[207]

As described by Verger et al.,^[107] the repulsive exciton–exciton interaction U originates from confinement of the exciton wavefunction and drives nonclassical generation through the so-called

“polariton blockade.” In this phenomenon, an increase in polariton density blueshifts the polariton resonance due to interactions between the excitonic components of the polaritons. A sufficiently strong blueshift, therefore, detunes the polariton resonance from the external excitation resonance (**Figure 6a**).^[208] Vividly, the presence of a few polaritons blocks the generation of further polaritons, thus photon antibunching occurs.

In CdSe colloidal QWs, namely, NPLs, confinement occurs in the out-of-plane direction and typically the in-plane exciton Bohr radius is comparable to the NPL’s thickness.^[108,109] Therefore, this system experiences appreciable exciton wavefunction confinement making it well suited to study for exciton–exciton interaction effects (the U term in Equation (5)). Yet it remains to accurately estimate the exciton–exciton interaction strength based on the properties of CdSe NPLs. Given that NPLs are 2D, it is reasonable to follow the discussion of Shahnazaryan et al. wherein the authors calculated the interaction strength of excitons in 2D semiconductor QWs.^[110] The interaction between two 2D excitons is given by the Hamiltonian matrix element

$$H_{XX} = \frac{e^2}{4\pi\epsilon} \frac{\lambda_{2D}}{A} I_{tot} \quad (6)$$

where e is the electron charge, ϵ is the material’s dielectric constant, λ_{2D} is the in-plane exciton Bohr radius, A is the in-plane area, and I_{tot} is the sum of the four coulomb interaction integrals. Realistically, it is sufficient to consider interactions between excitons with equal center of mass momenta, so by symmetry

$$I_{tot} = 2 (I_{dir} + I_{exch}^e) \quad (7)$$

where I_{dir} and I_{exch}^e are the direct and electron Coulomb exchange integrals, respectively.

The exciton–exciton interaction strength U is then calculated by taking the expectation value of H_{XX} using a 2D 1s hydrogenic approximation of the excitonic wave function. It is again realistic to consider the interaction in the limit of no momentum exchange between excitons, which yields the relatively simple formula for the interaction strength between two 1s excitons in a 2D structure^[209]

$$U \simeq \frac{3e^2}{\pi\epsilon} \frac{\lambda_{2D}}{A} \quad (8)$$

where the numerical pre-factor is derived from Monte Carlo calculations as given by Shahnazaryan et al. (Figure 6b),^[209] and the value is relatively insensitive to the effective electron and hole masses. For example, CdSe NPLs emitting at 585 nm with dimensions as reported by Cho et al.^[108] and with $\lambda_{2D} \simeq 1.2$ nm as reported by Brumberg^[109] yields $U \simeq 7.4$ meV. Experimentally, the polariton–polariton interaction has not yet been studied on the NPL platform to the best of our knowledge.

Optical studies have revealed that CdSe QDs have an attractive, rather than repulsive, exciton–exciton interaction.^[210] Given that a repulsive exciton–exciton interaction effectively drives optical nonlinearity, it is therefore crucial to tune the exciton–exciton interaction by controlling nanocrystal morphology and heterostructuring. Saba et al. experimentally investigated CdSe/CdS dot/rod heterostructures.^[211] These heterostructures combine strong electronic wavefunction confinement in the 0D CdSe dot

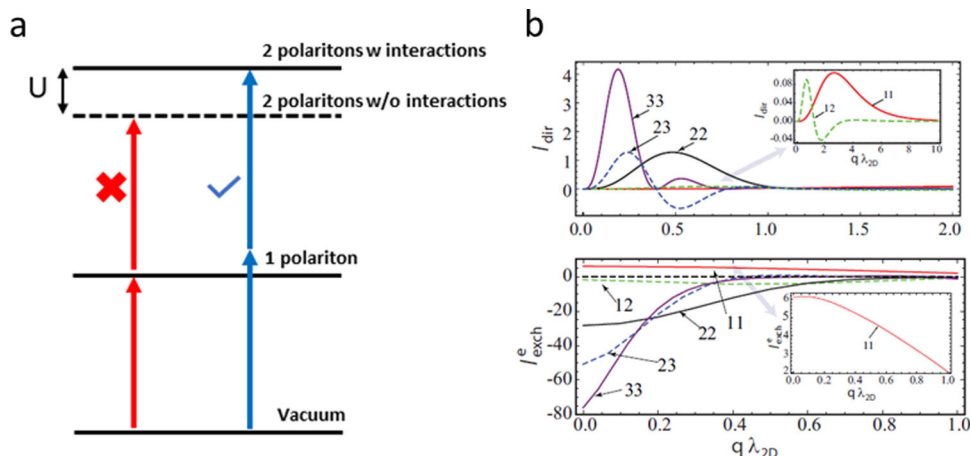


Figure 6. Single photon nonlinearity. a) Polariton blockade: The solid lines represent two-polariton state with nonzero nonlinearity, whereas the dotted lines represent the two-polariton state with zero nonlinearity.^[207] An increase in polariton density blueshifts the polariton resonance due to interactions between the excitonic components of the polaritons. The presence of a few polaritons blocks the generation of further polaritons, thus photon antibunching occurs.^[156] b) 2D exciton–exciton interaction: Monte Carlo calculation results of the interaction strength between s-type excitons with same (solid line) and different (dashed line) principal quantum numbers n as a function of scattered wave vector q .^[209] Figures are reprinted with permissions: b) Reproduced with permission.^[209] Copyright 2016, American Physical Society.

with strong absorption from the CdS rod shell. Blue-shifting of the PL peak under high pump fluences arises from the exciton–exciton interaction; this indicates tuning nanocrystal morphology can result in a stronger, repulsive exciton–exciton interaction.

Theoretical study suggests that core-shell II–VI nanocrystals with type II band alignment (i.e., staggered conduction and valence bands) have a large spatial separation between the electron and hole wavefunctions that generates strongly repulsive exciton–exciton interactions.^[212] For II–VI NPLs, careful modelling suggests core-crown CdSe/CdS nanoplatelets with type II band alignment can also achieve strong charge separation;^[213] however, the effect of this on the exciton–exciton interaction in these materials remains unexplored to the best of our knowledge. Therefore, further study of these NPL heterostructures and integration with optical cavities is warranted.

To further enhance the polariton–polariton interaction, it is promising to explore high-order Rydberg polaritons in a solution-processed material platform. The larger physical size of the Rydberg excitons results in a stronger polariton–polariton interaction. Bao et al. explored high-order Rydberg exciton–polaritons and their condensate in perovskites in a DBR cavity.^[111] The formation of Rydberg EPs in a single crystal CsPbBr₃ perovskite coupled to a DBR cavity was observed without any external fields. These Rydberg polaritons exhibit strong nonlinear behavior that leads to a coherent polariton condensate with a prominent blue shift.

4. Spin-Photon Interface

Solid-state spin qubits are a critical resource for QISE. By interfacing with “flying” photonic qubits they can help implement quantum memory and quantum repeaters, which are critical building blocks for quantum communication. They are also critical for quantum computing and quantum simulation, where the information will be encoded in the spin qubit. Many solid-state systems have been studied for such quantum spin-photon inter-

faces. While spin-states in a charged self-assembled QD were first proposed for quantum technologies,^[214–217] other defects with superior spin properties have emerged, namely different vacancy centers in diamond^[38] (including nitrogen vacancy and silicon vacancy), silicon vacancy centers in silicon carbide,^[218] and rare-earth doped crystals.^[219–221] However, the scalability of these material systems is still in question, and as such there is no clear winner on which material will provide the necessary scalability for quantum technologies while maintaining superior spin coherence times. Many colloidal materials are highly promising for spin-qubit development because they can be grown with ultra-high purity and are predominantly nuclear spin free. For example, ZnSe is 90% nuclear spin free and can be isotopically purified to better than 99.9%.^[222] However, the potential of these materials to host spin qubits has not been extensively studied, and there is a critical need for better fundamental understanding of the physics of various spin defects. As such, this remains one of the most under-studied aspects of solution-processed materials. Here we review the reported spin-physics in colloidal material systems and explore the potential for such systems for quantum applications.

Among many dopants in colloidal systems, lanthanides and transition metals are particularly promising for optically active spin qubits with long coherence times. Many examples of such impurities are known historically from investigations of these materials as phosphors.^[223] Both types of defects derive their spin properties from electrons in f and d orbitals that generally do not participate significantly in bonding. This leads to their decoupling from the environment and exceptionally long spin coherence times^[224,225] (approximately milli-seconds to second). We emphasize that this is an important consideration, and a major limitation of nitrogen-vacancy centers,^[56] especially when integrated with nanophotonic resonators. For similar reasons, internal optical transitions within the f and d shells are exceptionally narrow and have high quantum efficiency, albeit with small oscillator strengths.

Rare earth ions (REIs) are among the most studied optical centers in solids^[226] and these ion-doped crystals have recently emerged as a promising platform for quantum information processing. Possible applications of REI-doped crystals include optically interconnecting qubits to form a quantum network,^[7] quantum memories,^[227] quantum repeaters,^[228] and transduction from microwave superconducting qubits to photons at telecommunication frequencies.^[229,230] In addition, REI-doped crystals are naturally compatible with integrated nanophotonics as demonstrated recently.^[40,219,220,231–234] Triply ionized REIs (e.g., Yb³⁺ and Er³⁺) have a partially filled 4f shell that is shielded from the external environment by filled 5s² and 5p⁶ shells, and the dipole-forbidden 4f-4f transitions of the free ion span a broad range of frequencies from ultraviolet to infrared. Doping a host crystal with REIs splits the degeneracy of the free ion's states, resulting in a manifold of 4f states. Although the 4f-4f transitions are symmetry-forbidden in the free ion case, the point group symmetry of the host crystal field forces an odd parity symmetry component, which enables weak oscillator strengths for 4f-4f transitions between the ground and excited state manifolds. We note that there are also magnetic dipole transitions that are not symmetry forbidden. Crucially, these transitions have long lifetimes T_1 , long coherence lifetimes T_2 , and narrow homogeneous linewidths,^[235] for example, $T_1 \approx 1.9$ ms, $T_2 \approx 2.6$ ms, and $\Gamma_{\text{hom}} \approx 85$ Hz have been demonstrated in bulk Eu³⁺ doped Y₂SiO₅ at liquid helium temperature (4K). Furthermore, as pointed out by Thiel et al., one should target transitions between the lowest state of the ground state manifold and the lowest state of the excited state manifold in order to avoid non-radiative processes for the smallest homogeneous linewidth.^[228] The applicability of REI doped crystals for QISE follows from these characteristic manifolds of states.

One of the important quantum applications using REI doped crystal is transduction between microwave superconducting qubits and photons at telecommunication wavelength range for long-range quantum communication.^[229,236] Bartholomew et al. demonstrated microwave to optical transduction with Yb³⁺ doped yttrium orthovanadate crystal that was patterned into a monolithic waveguide. Degeneracy breaking of the excited ²F_{5/2} and ground ²F_{7/2} offers a portfolio of Λ -like and V-like energy level systems (Figure 7a). As an example of utilizing the V-like system for quantum transduction, an optical input at a frequency f_O pumps the atom from $|g_2\rangle$ to $|e_1\rangle$. The coherence generated on the spin transition from excitation at frequency f_M (connecting $|e_1\rangle$ to $|e_2\rangle$) is mapped to an optical coherence at frequency f_T (the transition from $|e_2\rangle$ to $|g_2\rangle$) through the optical pump field at f_O . Application of an external magnetic field can shift the energy level, and thus tuning the magnetic field in the range ≈ 0.5 –16 mT transduces microwave signals across ≈ 46 MHz with a bandwidth of ≈ 100 kHz (Figure 7b). A logical next step would be to couple to a cavity and increase the overall efficiency.^[236] Also in the solid state, Craiciu et al. demonstrated a photonic device consisting of a silicon Fabry–Perot cavity on Er³⁺ doped YOV with optical read/write of quantum memory at telecommunication wavelengths. Here the quantum memory storage protocol is based on the “atomic frequency comb protocol,” which exploits the inhomogeneous broadening of the dopant ion ensemble.^[237] By applying a DC electric field across the device with gold electrodes the ions' resonant frequencies can be Stark-shifted.

This will enable dynamic control of memory storage time and bandwidth. Craiciu et al. demonstrated on-demand memory storage times up to ≈ 400 ns, frequency tuning of ± 39 MHz, and bandwidth tuning in the range of 6–18 MHz (Figure 7c). Use of the optical cavity increases the overall efficiency of the device by enhancing the light-matter coupling.^[231]

In the examples so far, the nanophotonic devices were either monolithically fabricated from the REI doped crystal or the heterogeneous device was fabricated from a layer deposited on top of the REI doped crystal. In these top-down approaches, coupling to bulk REI doped crystals enables impressive coherence times T_2 ; however, their utility is hindered by the limited scalability of the platform. Additionally, it would be convenient to separately tune the emitter and the photonics. Therefore, we can consider a bottom-up approach in which solution-processed REI doped nanocrystals are integrated post-hoc with a prefabricated nanophotonic device. In addition to scalability, the nanoparticles offer a lower density of ions per volume preserving single qubit spectral selectivity, albeit at the cost of worse T_2 compared to the bulk.^[238]

Yb³⁺ doped CsPb(Cl_{1-x}Br_x)₃ perovskite nanocrystals have recently attracted attention in solar cell applications as a spectral downconverter via a quantum cutting mechanism.^[239] Strong absorption of a high energy optical photon by the host perovskite nanocrystal is followed by energy transfer to two Yb³⁺ defects in the host crystal structure, and emission of two near infrared photons through a 4f-4f transition in the Yb³⁺ ions.^[240,241] Like conventional REI doped crystals, Yb³⁺ doped perovskite nanocrystals have appealing spectral properties including strong absorption, narrow linewidth at cryogenic temperature, and efficient photoluminescence. Furthermore, spectroscopic measurements reveal strong crystal field splitting, resulting in a rich manifold of states viable for quantum information applications in either the Λ or V configurations (Figure 7d).^[242] Microwave to optical transduction in particular seems promising in this platform.^[243]

Interest in transition-metal impurities for QISE has emerged more recently. Promising experimental results include coherence times of 150 μ s for electron spins of Fe³⁺ in ZnO with prospects to reach the millisecond range with isotopic and chemical purification,^[244] coherence times of 68 μ s at low temperature (≈ 7 K) and 1 μ s at room temperature for transition metal complexes in molecular compounds,^[245] and longitudinal relaxation times of seconds for Mo⁵⁺ and V³⁺ in SiC.^[246]

The long lifetime of most optical transitions of lanthanide and transition metals has presented a challenge to addressing individual ions; the experiments listed above were all performed on impurity ensembles. Such ensemble spins could be useful for quantum memories or for quantum transduction. In recent years, researchers have demonstrated Mn²⁺ doped II-VI (CdSe, ZnSe, ZnO) QDs.^[247,248] Mn²⁺, a paramagnetic spin-5/2 system, exhibits both room temperature emission and electron-spin-resonance,^[249,250] a key element for a quantum-defect sensor, and strong interactions with the radiatively efficient QD exciton which can provide a path toward single optical spin readout. The excitonic interaction has been utilized to efficiently prepare the Mn²⁺ ensemble into a single spin state as well as to observe Larmor precession of the Mn²⁺ spins in a temperature of up to 40 K.^[250] Critically for elevated temperature operations, the spin-states of Mn²⁺ could be encoded into the polarization of the QD

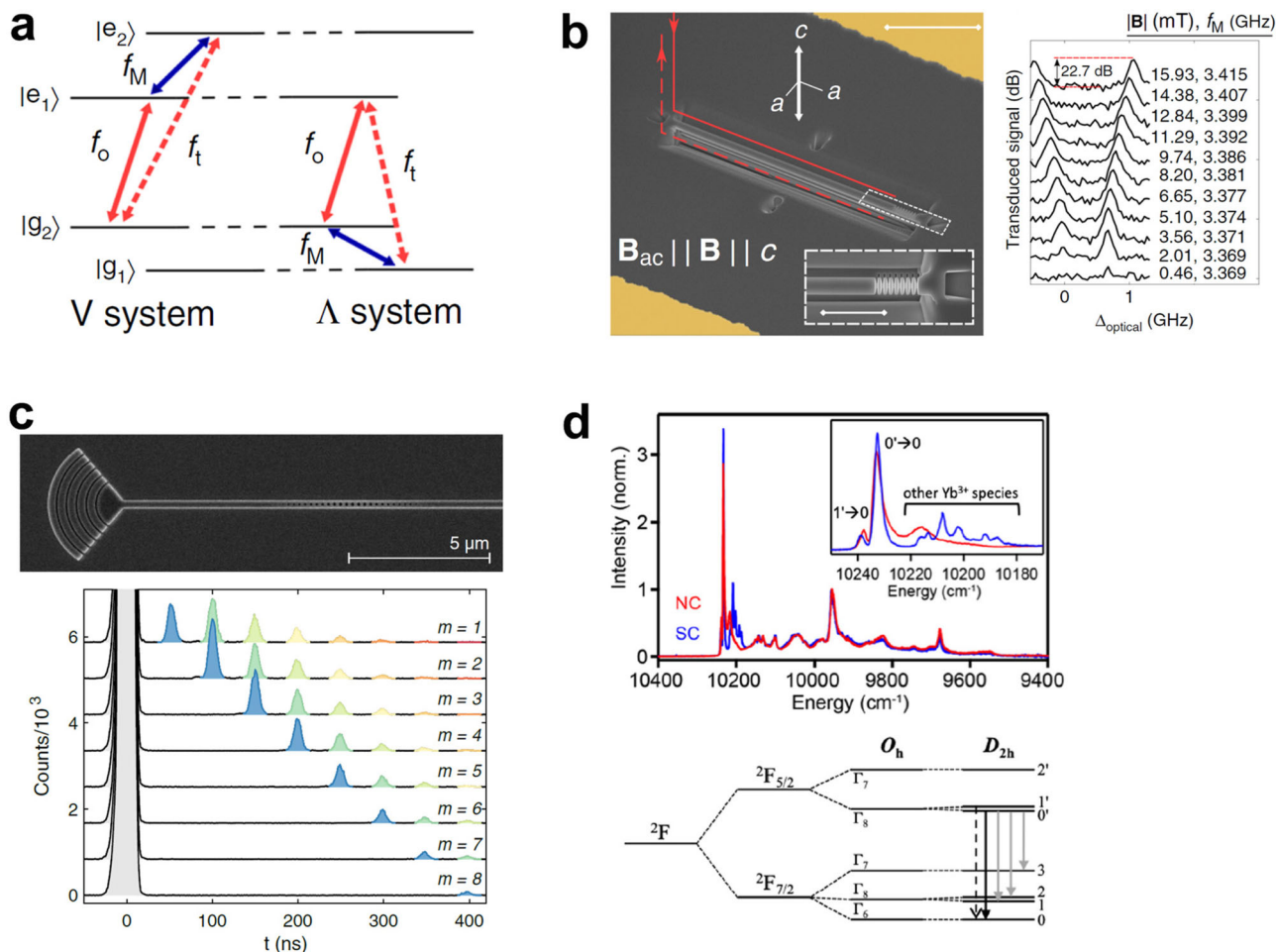


Figure 7. Spin-photon interface. a) Schematic of microwave to optical transduction with V-like and Λ -like energy level schemes.^[236] b) SEM of a monolithic Yb³⁺ doped YOY waveguide and demonstration of microwave to optical transduction.^[236] c) SEM of a silicon optical cavity evanescently coupled to underlying Er³⁺ doped YOY and temporal control of optical quantum memory read-out. Blue pulses indicate on-demand memory read-out.^[231] d) Photoluminescence spectrum of Yb³⁺ CsPbBr₃ perovskite nanocrystals at 5 K and a schematic of Yb³⁺ energy level splitting due to the perovskite on-site D_{2h} symmetry.^[242] Figures are reprinted with permissions: a,b) Reproduced with permission.^[236] Copyright 2020, Macmillan Publishers Ltd. c) Reproduced with permission.^[231] Copyright 2021, Optical Society of America. d) Reproduced with permission.^[242] Copyright 2020, American Physical Society.

exciton. At low temperatures, researchers have also utilized Mn²⁺ to perform nuclear spin resonance on spins functionalized to the surface of colloidal QDs.^[251]

5. Outlook

Scalable QISE technologies require extremely demanding performance, and as such there is no clear winner on what type of qubit will be most suitable. Similarly, for photonic quantum computing, there are many possible material systems with stringent requirements. While some of these materials, such as, self-assembled QDs or color centers in different crystalline materials are more well-studied, all of them face considerable bottlenecks for creating scalable fault-tolerant quantum technologies. Solution-processed materials are much less studied for QISE applications but have the benefit of easy scalability and the possibility of wafer-level integration using high-throughput semiconductor manufacturing processes. Hence, even though the quantum optical properties of these materials are not on par with current

state of the art quantum emitters, there is significant promise for synthetic chemistry to overcome these challenges. One important result will be to demonstrate indistinguishable single-photon emission from these emitters when deterministically integrated with nanophotonic structures. By interfering these single photons in large-scale photonic integrated circuits, different entangled states, including cluster states, can be created. Exciton-polaritons have already been demonstrated with many such colloidal emitters, with signatures of condensation and nonlinearity. However, the reported optical nonlinearities are far from the single photon nonlinear regime. Novel nanophotonic structures as well as novel emitters need to be designed to reach the quantum nonlinear regime. This includes engineering Rydberg states in these emitters and developing emitters with strong exciton-exciton interaction. Topological photonics and polaritonics could also be an interesting research direction. Recent advances in topological photonics have shown that exotic light-matter interactions can be realized by harnessing the topological protection of many body states resulting in photonic lattices with specially

designed energy momentum relationships.^[252,253] While microwave photons in a superconducting circuit platform have been used successfully to exhibit these unconventional cavity quantum electrodynamic effects, such demonstrations are missing in the optical domain.^[254] One of the principal bottlenecks faced by the topological photonics community is scalable integration of nonlinearities in the form of quantum emitters coupled to photonic cavity arrays. While the superconducting community has been successful in integrating qubits with the transmission line resonators in deterministic manner to achieve sufficiently strong nonlinearities, the photonics community, despite the inherent scalability of solid-state lattices, faces a few key challenges in similar integration of quantum emitters. First, to achieve strong nonlinear interactions in optics, we need to work with photonic lattices made up of high Q factor, low mode volume cavities with control over disorder.^[255] While different works in photonics have been successful in demonstrating topological phenomenon in photonic arrays,^[256] it is only recently that work on their design and fabrication with integration of quantum emitters in mind has taken place.^[257] Secondly, typical quantum emitters used in optics, like color centers, are not scalable. This is where the ability to deterministically position colloidal emitters could prove to be very useful for probing such effects. A combined system made of high Q, low mode volume photonic lattices with integrated colloidal emitters can be an ideal platform to study such unconventional topological phenomenon in optical domain. Finally, the spin physics in these colloidal systems are not well studied. While several dopants have been examined in colloidal systems, the quantum properties and spin-photon interfaces are underdeveloped. Future research directions will include finding materials with large ground state spin-coherence times and exploring the possibility of optical read-out of these spin-states. While many of these dopants exhibit superior properties in crystals, it remains to be seen how performance degrades in solution-processed materials. Understanding the reason for such degradation can also guide better synthesis techniques to improve the performance. Development of nanophotonic structures to interface with these spin-states will also constitute an important research direction.

Acknowledgements

This work was supported by NSF-QII-TAQS-1936100, NSF-1845009, and NSF MRSEC 1719797. The authors acknowledge helpful discussion with Prof. Andrei Faraon on QISE technologies using rare-earth-doped crystals.

Conflict of Interest

The authors declare no conflict of interest.

Data Availability Statement

The data that support the findings of this study are available from the corresponding author upon reasonable request.

Keywords

colloidal nanocrystals, nanophotonics, quantum optics

Received: June 8, 2021
Revised: October 17, 2021
Published online:

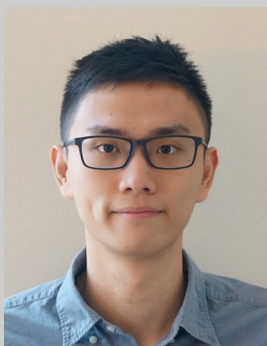
- [1] T. D. Ladd, F. Jelezko, R. Laflamme, Y. Nakamura, C. Monroe, J. L. O'Brien, *Nature* **2010**, *464*, 45.
- [2] F. Arute, K. Arya, R. Babbush, D. Bacon, J. C. Bardin, R. Barends, R. Biswas, S. Boixo, F. G. S. L. Brandao, D. A. Buell, B. Burkett, Y. Chen, Z. Chen, B. Chiaro, R. Collins, W. Courtney, A. Dunsworth, E. Farhi, B. Foxen, A. Fowler, C. Gidney, M. Giustina, R. Graff, K. Guerin, S. Habegger, M. P. Harrigan, M. J. Hartmann, A. Ho, M. Hoffmann, T. Huang, et al., *Nature* **2019**, *574*, 505.
- [3] Y. Nam, J.-S. Chen, N. C. Pienti, K. Wright, C. Delaney, D. Maslov, K. R. Brown, S. Allen, J. M. Amini, J. Apisdorf, K. M. Beck, A. Blinov, V. Chaplin, M. Chmielewski, C. Collins, S. Debnath, K. M. Hudek, A. M. Ducore, M. Keesan, S. M. Kreikemeier, J. Mizrahi, P. Solomon, M. Williams, J. D. Wong-Campos, D. Moehring, C. Monroe, J. Kim, *npj Quantum Inf.* **2020**, *6*, 33.
- [4] D. Maslov, Y. Nam, J. Kim, *Proc. IEEE* **2019**, *107*, 5.
- [5] J. M. Pino, J. M. Dreiling, C. Figgatt, J. P. Gaebler, S. A. Moses, M. S. Allman, C. H. Baldwin, M. Foss-Feig, D. Hayes, K. Mayer, C. Ryan-Anderson, B. Neyenhuis, *Nature* **2021**, *592*, 209.
- [6] A. S. Cacciapuoti, M. Caleffi, F. Tafuri, F. S. Cataliotti, S. Gherardini, G. Bianchi, *IEEE Network* **2020**, *34*, 137.
- [7] H. J. Kimble, *Nature* **2008**, *453*, 1023.
- [8] N. Lauk, N. Sinclair, S. Barzanjeh, J. P. Covey, M. Saffman, M. Spiropulu, C. Simon, *Quantum Sci. Technol.* **2020**, *5*, 020501.
- [9] J. L. O'Brien, A. Furusawa, J. Vučković, *Nat. Photonics* **2009**, *3*, 687.
- [10] J. M. Arrazola, V. Bergholm, K. Brádler, T. R. Bromley, M. J. Collins, I. Dhand, A. Fumagalli, T. Gerrits, A. Goussev, L. G. Helt, J. Hundal, T. Isacsson, R. B. Israel, J. Izaac, S. Jahangiri, R. Janik, N. Killoran, S. P. Kumar, J. Lavoie, A. E. Lita, D. H. Mahler, M. Menotti, B. Morrison, S. W. Nam, L. Neuhaus, H. Y. Qi, N. Quesada, A. Repping, K. K. Sabapathy, M. Schuld, et al., *Nature* **2021**, *591*, 54.
- [11] H. S. Zhong, H. Wang, Y. H. Deng, M. C. Chen, L. C. Peng, Y. H. Luo, J. Qin, D. Wu, X. Ding, Y. Hu, P. Hu, X. Y. Yang, W. J. Zhang, H. Li, Y. Li, X. Jiang, L. Gan, G. Yang, L. You, Z. Wang, L. Li, N. Le Liu, C. Y. Lu, J. W. Pan, *Science* **2021**, *370*, 1460.
- [12] S. Takeda, A. Furusawa, *APL Photonics* **2019**, *4*, 060902.
- [13] T. Rudolph, *APL Photonics* **2017**, *2*, 030901.
- [14] J. Wang, S. Paesani, Y. Ding, R. Santagati, P. Skrzypczyk, A. Salavrakos, J. Tura, R. Augusiak, L. Mančinska, D. Bacco, D. Bonneau, J. W. Silverstone, Q. Gong, A. Acín, K. Rottwitz, L. K. Oxenløwe, J. L. O'Brien, A. Laing, M. G. Thompson, *Science* **2018**, *360*, 285.
- [15] S. Buckley, K. Rivoire, J. Vučković, *Rep. Prog. Phys.* **2012**, *75*, 126503.
- [16] Y.-M. He, Y. He, Y.-J. Wei, D. Wu, M. Atatüre, C. Schneider, S. Höfling, M. Kamp, C.-Y. Lu, J.-W. Pan, *Nat. Nanotechnol.* **2013**, *8*, 213.
- [17] N. Somaschi, V. Giesz, L. De Santis, J. C. Lored, M. P. Almeida, G. Hornecker, S. L. Portalupi, T. Grange, C. Antón, J. Demory, C. Gómez, I. Sagnes, N. D. Lanzillotti-Kimura, A. Lemaître, A. Auffèves, A. G. White, L. Lanco, P. Senellart, *Nat. Photonics* **2016**, *10*, 340.
- [18] X. Ding, Y. He, Z.-C. Duan, N. Gregersen, M.-C. Chen, S. Unsleber, S. Maier, C. Schneider, M. Kamp, S. Höfling, C.-Y. Lu, J.-W. Pan, *Phys. Rev. Lett.* **2016**, *116*, 020401.
- [19] P. Senellart, G. Solomon, A. White, *Nat. Nanotechnol.* **2017**, *12*, 1026.
- [20] H. Wang, Y.-M. He, T.-H. Chung, H. Hu, Y. Yu, S. Chen, X. Ding, M.-C. Chen, J. Qin, X. Yang, R.-Z. Liu, Z.-C. Duan, J.-P. Li, S. Gerhardt, K. Winkler, J. Jurkat, L.-J. Wang, N. Gregersen, Y.-H. Huo, Q. Dai, S. Yu, S. Höfling, C.-Y. Lu, J.-W. Pan, *Nat. Photonics* **2019**, *13*, 770.
- [21] N. Tomm, A. Javadi, N. O. Antoniadis, D. Najer, M. C. Löbl, A. R. Korsch, R. Schott, S. R. Valentin, A. D. Wieck, A. Ludwig, R. J. Warburton, *Nat. Nanotechnol.* **2021**, *16*, 399.
- [22] S. Rodt, S. Reitzenstein, *APL Photonics* **2021**, *6*, 010901.
- [23] F. Albert, S. Stobbe, C. Schneider, T. Heindel, S. Reitzenstein, S. Höfling, P. Lodahl, L. Worschech, A. Forchel, *Appl. Phys. Lett.* **2010**, *96*, 151102.

- [24] A. Dousse, L. Lanco, J. Suffczyński, E. Semenova, A. Miard, A. Lemaître, I. Sagnes, C. Roblin, J. Bloch, P. Senellart, *Phys. Rev. Lett.* **2008**, *101*, 267404.
- [25] M. Gschrey, F. Gericke, A. Schüßler, R. Schmidt, J.-H. Schulze, T. Heindel, S. Rodt, A. Strittmatter, S. Reitzenstein, *Appl. Phys. Lett.* **2013**, *102*, 251113.
- [26] J.-H. Kim, S. Aghaeimeibodi, C. J. K. Richardson, R. P. Leavitt, D. Englund, E. Waks, *Nano Lett.* **2017**, *17*, 7394.
- [27] M. Davanco, J. Liu, L. Sapienza, C.-Z. Zhang, J. V. D. M. Cardoso, V. Verma, R. Mirin, S. W. Nam, L. Liu, K. Srinivasan, *Nat. Commun.* **2017**, *8*, 889.
- [28] J. P. Reithmaier, G. Şek, A. Löffler, C. Hofmann, S. Kuhn, S. Reitzenstein, L. V. Keldysh, V. D. Kulakovskii, T. L. Reinecke, A. Forchel, *Nature* **2004**, *432*, 197.
- [29] F. Ding, R. Singh, J. D. Plumhof, T. Zander, V. Křápek, Y. H. Chen, M. Benyoucef, V. Zwiller, K. Dörr, G. Bester, A. Rastelli, O. G. Schmidt, *Phys. Rev. Lett.* **2010**, *104*, 067405.
- [30] M. Schmidt, M. V. Helversen, S. Fischbach, A. Kaganskiy, R. Schmidt, A. Schliwa, T. Heindel, S. Rodt, S. Reitzenstein, *Opt. Mater. Express* **2020**, *10*, 76.
- [31] S. Reitzenstein, S. Münch, P. Franeck, A. Rahimi-Iman, A. Löffler, S. Höfling, L. Worschech, A. Forchel, *Phys. Rev. Lett.* **2009**, *103*, 127401.
- [32] C. Kistner, T. Heindel, C. Schneider, A. Rahimi-Iman, S. Reitzenstein, S. Höfling, A. Forchel, *Opt. Express* **2008**, *16*, 15006.
- [33] A. J. Bennett, R. B. Patel, J. Skiba-Szymanska, C. A. Nicoll, I. Farrer, D. A. Ritchie, A. J. Shields, *Appl. Phys. Lett.* **2010**, *97*, 031104.
- [34] M. Heuck, K. Jacobs, D. R. Englund, *Phys. Rev. Lett.* **2020**, *124*, 160501.
- [35] L. M. Duan, H. J. Kimble, *Phys. Rev. Lett.* **2004**, *92*, 127902.
- [36] A. Faraon, I. Fushman, D. Englund, N. Stoltz, P. Petroff, J. Vučković, *Nat. Phys.* **2008**, *4*, 859.
- [37] A. Majumdar, M. Bajcsy, J. Vučković, *Phys. Rev. A* **2012**, *85*, 041801.
- [38] C. Bradac, W. Gao, J. Forneris, M. E. Trusheim, I. Aharonovich, *Nat. Commun.* **2019**, *10*, 5625.
- [39] M. Radulaski, M. Widmann, M. Niethammer, J. L. Zhang, S. Y. Lee, T. Rendler, K. G. Lagoudakis, N. T. Son, E. Jánzén, T. Ohshima, J. Wrachtrup, J. Vučković, *Nano Lett.* **2017**, *17*, 1782.
- [40] T. Zhong, J. M. Kindem, J. G. Bartholomew, J. Rochman, I. Craiciu, V. Verma, S. W. Nam, F. Marsili, M. D. Shaw, A. D. Beyer, A. Faraon, *Phys. Rev. Lett.* **2018**, *121*, 183603.
- [41] N. P. de Leon, K. M. Itoh, D. Kim, K. K. Mehta, T. E. Northup, H. Paik, B. S. Palmer, N. Samarth, S. Sangtawesin, D. W. Steuerman, *Science* **2021**, *372*, eabb2823.
- [42] C. R. Kagan, L. C. Bassett, C. B. Murray, S. M. Thompson, *Chem. Rev.* **2021**, *121*, 3186.
- [43] D. Zherebetsky, M. Scheele, Y. Zhang, N. Bronstein, C. Thompson, D. Britt, M. Salmeron, P. Alivisatos, L. W. Wang, *Science* **2014**, *344*, 1380.
- [44] B. Guzelurk, Y. Kelestemur, K. Gungor, A. Yeltik, M. Z. Akgul, Y. Wang, R. Chen, C. Dang, H. Sun, H. V. Demir, *Adv. Mater.* **2015**, *27*, 2741.
- [45] M. Bayer, *Ann. Phys.* **2019**, *531*, 1900039.
- [46] D. M. Kroupa, M. Vörös, N. P. Brawand, B. W. McNichols, E. M. Miller, J. Gu, A. J. Nozik, A. Sellinger, G. Galli, M. C. Beard, *Nat. Commun.* **2017**, *8*, 15257.
- [47] H. Utzat, W. Sun, A. E. K. Kaplan, F. Krieg, M. Ginterseder, B. Spokoynny, N. D. Klein, K. E. Shulenberger, C. F. Perkinson, M. V. Kovalenko, M. G. Bawendi, *Science* **2019**, *363*, 1068.
- [48] Y. Shirasaki, G. J. Supran, M. G. Bawendi, V. Bulović, *Nat. Photonics* **2013**, *7*, 13.
- [49] Z. Yang, M. Gao, W. Wu, X. Yang, X. W. Sun, J. Zhang, H. C. Wang, R. S. Liu, C. Y. Han, H. Yang, W. Li, *Mater. Today* **2019**, *24*, 69.
- [50] S. Wu, S. Buckley, J. R. Schaibley, L. Feng, J. Yan, D. G. Mandrus, F. Hatami, W. Yao, J. Vučković, A. Majumdar, X. Xu, *Nature* **2015**, *520*, 69.
- [51] T. K. Fryett, Y. Chen, J. Whitehead, Z. M. Peycke, X. Xu, A. Majumdar, *ACS Photonics* **2018**, *5*, 2176.
- [52] R. Su, C. Diederichs, J. Wang, T. C. H. Liew, J. Zhao, S. Liu, W. Xu, Z. Chen, Q. Xiong, *Nano Lett.* **2017**, *17*, 3982.
- [53] Y. Chen, S. Miao, T. Wang, D. Zhong, A. Saxena, C. Chow, J. Whitehead, D. Gerace, X. Xu, S. F. Shi, A. Majumdar, *Nano Lett.* **2020**, *20*, 5292.
- [54] N. H. M. Dang, D. Gerace, E. Drouard, G. Trippé-Allard, F. Lédeé, R. Mazurczyk, E. Deleporte, C. Seassal, H. S. Nguyen, *Nano Lett.* **2020**, *20*, 2113.
- [55] A. Majumdar, A. Rundquist, M. Bajcsy, J. Vučković, *Phys. Rev. B: Condens. Matter Mater. Phys.* **2012**, *86*, 045315.
- [56] T. Zhong, J. M. Kindem, E. Miyazono, A. Faraon, *Nat. Commun.* **2015**, *6*, 8206.
- [57] Y. Chen, J. Whitehead, A. Ryou, J. Zheng, P. Xu, T. Fryett, A. Majumdar, *Opt. Lett.* **2019**, *44*, 3058.
- [58] X. Wu, T. Fan, A. A. Eftekhar, A. Adibi, *Opt. Lett.* **2019**, *44*, 4941.
- [59] L. Protesescu, S. Yakunin, M. I. Bodnarchuk, F. Krieg, R. Caputo, C. H. Hendon, R. X. Yang, A. Walsh, M. V. Kovalenko, *Nano Lett.* **2015**, *15*, 3692.
- [60] V. Chandrasekaran, M. D. Tessier, D. Dupont, P. Geiregat, Z. Hens, E. Brainis, *Nano Lett.* **2017**, *17*, 6104.
- [61] H. Gargoubi, T. Guillet, S. Jaziri, J. Balti, B. Guizal, *Phys. Rev. E* **2016**, *94*, 043310.
- [62] A. Majumdar, P. Kaer, M. Bajcsy, E. D. Kim, K. G. Lagoudakis, A. Rundquist, J. Vučković, *Phys. Rev. Lett.* **2013**, *111*, 027402.
- [63] P. Kok, H. Lee, J. P. Dowling, *Phys. Rev. A: At., Mol., Opt. Phys.* **2002**, *65*, 5.
- [64] A. Faraon, A. Majumdar, D. Englund, E. Kim, M. Bajcsy, J. Vučković, *New J. Phys.* **2011**, *13*, 055025.
- [65] J. Carolan, C. Harrold, C. Sparrow, E. Martín-López, N. J. Russell, J. W. Silverstone, P. J. Shadbolt, N. Matsuda, M. Oguma, M. Itoh, G. D. Marshall, M. G. Thompson, J. C. F. Matthews, T. Hashimoto, J. L. O'Brien, A. Laing, *Science* **2015**, *349*, 711.
- [66] J. B. Spring, B. J. Metcalf, P. C. Humphreys, W. S. Kolthammer, X. M. Jin, M. Barbieri, A. Datta, N. Thomas-Peter, N. K. Langford, D. Kundys, J. C. Gates, B. J. Smith, P. G. R. Smith, I. A. Walmsley, *Science* **2013**, *339*, 798.
- [67] C. Ma, X. Wang, V. Anant, A. D. Beyer, M. D. Shaw, S. Mookherjea, *Opt. Express* **2017**, *25*, 32995.
- [68] K. Rivoire, S. Buckley, A. Majumdar, H. Kim, P. Petroff, J. Vučković, *Appl. Phys. Lett.* **2011**, *98*, 083105.
- [69] H. Wang, Y. He, Y.-H. Li, Z.-E. Su, B. Li, H.-L. Huang, X. Ding, M.-C. Chen, C. Liu, J. Qin, J.-P. Li, Y.-M. He, C. Schneider, M. Kamp, C.-Z. Peng, S. Höfling, C.-Y. Lu, J.-W. Pan, *Nat. Photonics* **2017**, *11*, 361.
- [70] H. Wang, J. Qin, X. Ding, M. C. Chen, S. Chen, X. You, Y. M. He, X. Jiang, L. You, Z. Wang, C. Schneider, J. J. Renema, S. Höfling, C. Y. Lu, J. W. Pan, *Phys. Rev. Lett.* **2019**, *123*, 250503.
- [71] J. Große, M. von Helversen, A. Koulas-Simos, M. Hermann, S. Reitzenstein, *APL Photonics* **2020**, *5*, 096107.
- [72] J. Zhang, Q. Huang, L. Jordao, S. Chattaraj, S. Lu, A. Madhukar, *APL Photonics* **2020**, *5*, 116106.
- [73] M. Felici, P. Gallo, A. Mohan, B. Dwir, A. Rudra, E. Kapon, *Small* **2009**, *5*, 938.
- [74] K. A. Atlasov, M. Calic, K. F. Karlsson, P. Gallo, A. Rudra, B. Dwir, E. Kapon, *Opt. Express* **2009**, *17*, 18178.
- [75] M. Calic, P. Gallo, M. Felici, K. A. Atlasov, B. Dwir, A. Rudra, G. Biassiol, L. Sorba, G. Tarel, V. Savona, E. Kapon, *Phys. Rev. Lett.* **2011**, *106*, 227402.
- [76] T. Sünnner, C. Schneider, M. Strauß, A. Huggenberger, D. Wiener, S. Höfling, M. Kamp, A. Forchel, *Opt. Lett.* **2008**, *33*, 1759.

- [77] C. Schneider, T. Heindel, A. Huggenberger, P. Weinmann, C. Kistner, M. Kamp, S. Reitzenstein, S. Höfling, A. Forchel, *Appl. Phys. Lett.* **2009**, *94*, 111111.
- [78] A. Kaganskiy, F. Gericke, T. Heuser, T. Heindel, X. Porte, S. Reitzenstein, *Appl. Phys. Lett.* **2018**, *112*, 071101.
- [79] I. Aharonovich, D. Englund, M. Toth, *Nat. Photonics* **2016**, *10*, 631.
- [80] T. M. Babinec, B. J. M. Hausmann, M. Khan, Y. Zhang, J. R. Maze, P. R. Hemmer, M. Lončar, *Nat. Nanotechnol.* **2010**, *5*, 195.
- [81] N. H. Wan, T. J. Lu, K. C. Chen, M. P. Walsh, M. E. Trusheim, L. De Santis, E. A. Bersin, I. B. Harris, S. L. Mouradian, I. R. Christen, E. S. Bielejec, D. Englund, *Nature* **2020**, *583*, 226.
- [82] V. Wood, V. Bulović, *Nano Rev.* **2010**, *1*, 5202.
- [83] K. S. Cho, E. K. Lee, W. J. Joo, E. Jang, T. H. Kim, S. J. Lee, S. J. Kwon, J. Y. Han, B. K. Kim, B. L. Choi, J. M. Kim, *Nat. Photonics* **2009**, *3*, 341.
- [84] H. Deschout, F. C. Zanacchi, M. Młodzianoski, A. Diaspro, J. Bewersdorf, S. T. Hess, K. Braeckmans, *Nat. Methods* **2014**, *11*, 253.
- [85] M. O. Scully, M. S. Zubairy, I. A. Walmsley, *Am. J. Phys.* **1999**, *67*, 648.
- [86] X. Brokmann, G. Messin, P. Desbiolles, E. Giacobino, M. Dahan, J. P. Hermier, *New J. Phys.* **2004**, *6*, 99.
- [87] X. Lin, X. Dai, C. Pu, Y. Deng, Y. Niu, L. Tong, W. Fang, Y. Jin, X. Peng, *Nat. Commun.* **2017**, *8*, 1132.
- [88] G. Yuan, D. E. Gómez, N. Kirkwood, K. Boldt, P. Mulvaney, *ACS Nano* **2018**, *12*, 3397.
- [89] Y. Chen, J. Vela, H. Htoon, J. L. Casson, D. J. Werder, D. A. Bussian, V. I. Klimov, J. A. Hollingsworth, *J. Am. Chem. Soc.* **2008**, *130*, 5026.
- [90] V. Fomento, D. J. Nesbitt, *Nano Lett.* **2008**, *8*, 287.
- [91] S. Hohng, T. Ha, *J. Am. Chem. Soc.* **2004**, *126*, 1324.
- [92] S. D. Quinn, A. Rafferty, E. Dick, M. J. Morten, F. J. Kettles, C. Knox, M. Murrie, S. W. Magennis, *J. Phys. Chem. C* **2016**, *120*, 19487.
- [93] Y. S. Park, S. Guo, N. S. Makarov, V. I. Klimov, *ACS Nano* **2015**, *9*, 10386.
- [94] T. Huang, P. Han, X. Wang, S. Feng, W. Sun, J. Ye, Y. Zhang, *Superlattices Microstruct.* **2016**, *92*, 52.
- [95] A. V. Kuhlmann, J. Houel, A. Ludwig, L. Greuter, D. Reuter, A. D. Wieck, M. Poggio, R. J. Warburton, *Nat. Phys.* **2013**, *9*, 570.
- [96] F. W. Sun, C. W. Wong, *Phys. Rev. A: At., Mol., Opt. Phys.* **2009**, *79*, 013824.
- [97] T. Grange, G. Hornecker, D. Hunger, J. P. Poizat, J. M. Gérard, P. Senellart, A. Auffèves, *Phys. Rev. Lett.* **2015**, *114*, 193601.
- [98] S. Gupta, E. Waks, *Opt. Express* **2013**, *21*, 29612.
- [99] Z. Yang, M. Pelton, M. I. Bodnarchuk, M. V. Kovalenko, E. Waks, *Appl. Phys. Lett.* **2017**, *111*, 221104.
- [100] C. F. Fong, Y. Yin, Y. Chen, D. Rosser, J. Xing, A. Majumdar, Q. Xiong, *Opt. Express* **2019**, *27*, 18673.
- [101] K. J. Vahala, *Nature* **2003**, *424*, 839.
- [102] A. Saxena, Y. Chen, A. Ryou, C. G. Sevilla, P. Xu, A. Majumdar, *ACS Photonics* **2019**, *6*, 3166.
- [103] H. Choi, D. Zhu, Y. Yoon, D. Englund, *Phys. Rev. Lett.* **2019**, *122*, 183602.
- [104] C. Santori, D. Fattal, J. Vučković, G. S. Solomon, Y. Yamamoto, *Nature* **2002**, *419*, 594.
- [105] F. Liu, A. J. Brash, J. O'Hara, L. M. P. P. Martins, C. L. Phillips, R. J. Coles, B. Royall, E. Clarke, C. Bentham, N. Prtljaga, I. E. Itskevich, L. R. Wilson, M. S. Skolnick, A. M. Fox, *Nat. Nanotechnol.* **2018**, *13*, 835.
- [106] G. Kiršanske, H. Thyrrerstrup, R. S. Daveau, C. L. Dreeßen, T. Pregnolato, L. Midolo, P. Tighineanu, A. Javadi, S. Stobbe, R. Schott, A. Ludwig, A. D. Wieck, S. I. Park, J. D. Song, A. V. Kuhlmann, I. Söllner, M. C. Löbl, R. J. Warburton, P. Lodahl, *Phys. Rev. B* **2017**, *96*, 165306.
- [107] H. Wang, J. Qin, X. Ding, M. C. Chen, S. Chen, X. You, Y. M. He, X. Jiang, L. You, Z. Wang, C. Schneider, J. J. Renema, S. Höfling, C. Y. Lu, J. W. Pan, *Phys. Rev. Lett.* **2019**, *123*, 250503.
- [108] N. Akopian, N. H. Lindner, E. Poem, Y. Berlatzky, J. Avron, D. Gershoni, B. D. Gerardot, P. M. Petroff, *Phys. Rev. Lett.* **2006**, *96*, 130501.
- [109] J. Liu, R. Su, Y. Wei, B. Yao, S. F. C. da Silva, Y. Yu, J. Iles-Smith, K. Srinivasan, A. Rastelli, J. Li, X. Wang, *Nat. Nanotechnol.* **2019**, *14*, 586.
- [110] I. Fushman, D. Englund, J. Vučković, *Appl. Phys. Lett.* **2005**, *87*, 241102.
- [111] C. A. Foell, E. Schelew, H. Qiao, K. A. Abel, S. Hughes, F. C. J. M. van Veggel, J. F. Young, *Opt. Express* **2012**, *20*, 10453.
- [112] F. Biccari, A. Boschetti, G. Pettinari, F. L. China, M. Gurioli, F. Intonti, A. Vinattieri, M. Sharma, M. Capizzi, A. Gerardino, L. Businaro, M. Hopkinson, A. Polimeni, M. Felici, *Adv. Mater.* **2018**, *30*, 1705450.
- [113] Y. Chen, A. Ryou, M. R. Friedfeld, T. Fryett, J. Whitehead, B. M. Cos-sairt, A. Majumdar, *Nano Lett.* **2018**, *18*, 6404.
- [114] W. Xie, R. Gomes, T. Aubert, S. Bisschop, Y. Zhu, Z. Hens, E. Brainis, D. Van Thourhout, *Nano Lett.* **2015**, *15*, 7481.
- [115] A. Eich, T. C. Spiekermann, H. Gehring, L. Sommer, J. R. Bankwitz, P. P. J. Schrinner, J. A. Preus, S. M. de Vasconcelos, R. Bratschitsch, W. H. P. Pernice, C. Schuck, arXiv:2104.11830v1, **2021**.
- [116] W. Xie, R. Gomes, T. Aubert, S. Bisschop, Y. Zhu, Z. Hens, E. Brainis, D. Van Thourhout, *Nano Lett.* **2015**, *15*, 7481.
- [117] J. E. Fröch, S. Kim, C. Stewart, X. Xu, Z. Du, M. Lockrey, M. Toth, I. Aharonovich, *Nano Lett.* **2020**, *20*, 2784.
- [118] K. C. Smith, Y. Chen, A. Majumdar, D. J. Masiello, *Phys. Rev. Appl.* **2020**, *13*, 044041.
- [119] L. Zhang, B. Lv, H. Yang, R. Xu, X. Wang, M. Xiao, Y. Cui, J. Zhang, *Nanoscale* **2019**, *11*, 12619.
- [120] K. Park, Z. Deutsch, J. J. Li, D. Oron, S. Weiss, *ACS Nano* **2012**, *6*, 10013.
- [121] G. Walters, M. Wei, O. Voznyy, R. Quintero-Bermudez, A. Kiani, D.-M. Smilgies, R. Munir, A. Amassian, S. Hoogland, E. Sargent, *Nat. Commun.* **2018**, *9*, 4214.
- [122] S. A. Empedocles, M. G. Bawendi, *Science* **1997**, *278*, 2114.
- [123] C. Matthiesen, A. N. Vamvakas, M. Atatüre, *Phys. Rev. Lett.* **2012**, *108*, 093602.
- [124] A. Faraon, A. Majumdar, J. Vučković, *Phys. Rev. A* **2010**, *81*, 033838.
- [125] D. Englund, A. Majumdar, A. Faraon, M. Toishi, N. Stoltz, P. Petroff, J. Vučković, *Phys. Rev. Lett.* **2010**, *104*, 073904.
- [126] R. M. Ma, R. F. Oulton, *Nat. Nanotechnol.* **2019**, *14*, 12.
- [127] P. Munnely, T. Heindel, A. Thoma, M. Kamp, S. Höfling, C. Schneider, S. Reitzenstein, *ACS Photonics* **2017**, *4*, 790.
- [128] S. Kreinberg, T. Grbešić, M. Strauß, A. Carmele, M. Emmerling, C. Schneider, S. Höfling, X. Porte, S. Reitzenstein, *Light: Sci. Appl.* **2018**, *7*, 41.
- [129] Y. S. Park, J. Roh, B. T. Diroll, R. D. Schaller, V. I. Klimov, *Nat. Rev. Mater.* **2021**, *6*, 382.
- [130] P. Geiregat, D. Van Thourhout, Z. Hens, *NPG Asia Mater.* **2019**, *11*, 1234567890.
- [131] C. Dang, J. Lee, C. Breen, J. S. Steckel, S. Coe-Sullivan, A. Nurmikko, *Nat. Nanotechnol.* **2012**, *7*, 335.
- [132] V. I. Klimov, A. A. Mikhailovsky, S. Xu, A. Malko, J. A. Hollingsworth, C. A. Leatherdale, H. J. Eisler, M. G. Bawendi, *Science* **2000**, *290*, 314.
- [133] Y. Wang, V. D. Ta, K. S. Leck, B. H. I. Tan, Z. Wang, T. He, C. D. Ohl, H. V. Demir, H. Sun, *Nano Lett.* **2017**, *17*, 2640.
- [134] K. Rong, C. Sun, K. Shi, Q. Gong, J. Chen, *ACS Photonics* **2017**, *4*, 1776.
- [135] X. Yang, B. Li, *ACS Macro Lett.* **2014**, *3*, 1266.
- [136] F. Montanarella, D. Urbonas, L. Chadwick, P. G. Moerman, P. J. Baesjou, R. F. Mahrt, A. Van Blaaderen, T. Stöferle, D. Vanmaekelbergh, *ACS Nano* **2018**, *12*, 12788.
- [137] W. Xie, T. Stöferle, G. Rainò, T. Aubert, S. Bisschop, Y. Zhu, R. F. Mahrt, P. Geiregat, E. Brainis, Z. Hens, D. Van Thourhout, *Adv. Mater.* **2017**, *29*, 1604866.

- [138] B. Le Feber, F. Prins, E. De Leo, F. T. Rabouw, D. J. Norris, *Nano Lett.* **2018**, *18*, 1028.
- [139] P. J. Cegielski, A. L. Giesecke, S. Neutzner, C. Porschatis, M. Gandini, D. Schall, C. A. R. Perini, J. Bolten, S. Suckow, S. Kataria, B. Chmielak, T. Wahlbrink, A. Petrozza, M. C. Lemme, *Nano Lett.* **2018**, *18*, 6915.
- [140] R. M. Ma, R. F. Oulton, *Nat. Nanotechnol.* **2019**, *14*, 12.
- [141] Y. Zhu, W. Xie, S. Bisschop, T. Aubert, E. Brainis, P. Geiregat, Z. Hens, D. Van Thourhout, *ACS Photonics* **2017**, *4*, 2446.
- [142] Z. He, B. Chen, Y. Hua, Z. Liu, Y. Wei, S. Liu, A. Hu, X. Shen, Y. Zhang, Y. Gao, J. Liu, *Adv. Opt. Mater.* **2020**, *8*, 2000453.
- [143] P. J. Cegielski, A. L. Giesecke, S. Neutzner, C. Porschatis, M. Gandini, D. Schall, C. A. R. Perini, J. Bolten, S. Suckow, S. Kataria, B. Chmielak, T. Wahlbrink, A. Petrozza, M. C. Lemme, *Nano Lett.* **2018**, *18*, 6915.
- [144] F. Fan, O. Voznyy, R. P. Sabatini, K. T. Bicanic, M. M. Adachi, J. R. McBride, K. R. Reid, Y. S. Park, X. Li, A. Jain, R. Quintero-Bermudez, M. Saravanapavanantham, M. Liu, M. Korkusinski, P. Hawrylak, V. I. Klimov, S. J. Rosenthal, S. Hoogland, E. H. Sargent, *Nature* **2017**, *544*, 75.
- [145] M. Pelton, *J. Phys. Chem. C* **2018**, *122*, 10659.
- [146] C. She, I. Fedin, D. S. Dolzhenkov, A. Demortière, R. D. Schaller, M. Pelton, D. V. Talapin, *Nano Lett.* **2014**, *14*, 2772.
- [147] J. Q. Grim, S. Christodoulou, F. Di Stasio, R. Krahn, R. Cingolani, L. Manna, I. Moreels, *Nat. Nanotechnol.* **2014**, *9*, 891.
- [148] Z. Yang, M. Pelton, I. Fedin, D. V. Talapin, E. Waks, *Nat. Commun.* **2017**, *8*, 143.
- [149] Q. Zeng, E. Lafalce, C. H. Lin, M. J. Smith, J. Jung, Y. Yoon, Z. Lin, V. V. Tsukruk, Z. V. Vardeny, *Nano Lett.* **2019**, *19*, 6049.
- [150] E. Lafalce, Q. Zeng, C. H. Lin, M. J. Smith, S. T. Malak, J. Jung, Y. J. Yoon, Z. Lin, V. V. Tsukruk, Z. V. Vardeny, *Nat. Commun.* **2019**, *10*, 561.
- [151] J. Yu, S. Shendrey, W. kyu Koh, B. Liu, M. Li, S. Hou, C. Hettiarachchi, S. Delikanli, P. Hernández-Martínez, M. D. Birowosuto, H. Wang, T. C. Sum, H. V. Demir, C. Dang, *Sci. Adv.* **2019**, *5*, eaav3140.
- [152] J. Roh, Y. S. Park, J. Lim, V. I. Klimov, *Nat. Commun.* **2020**, *11*, 271.
- [153] H. M. Gibbs, G. Khitrova, S. W. Koch, *Nat. Photonics* **2011**, *5*, 273.
- [154] D. E. Chang, V. Vuletić, M. D. Lukin, *Nat. Photonics* **2014**, *8*, 685.
- [155] I. Carusotto, C. Ciuti, *Rev. Mod. Phys.* **2013**, *85*, 299.
- [156] D. Gerace, F. Laussy, D. Sanvitto, *Nat. Mater.* **2019**, *18*, 200.
- [157] T. Byrnes, N. Y. Kim, Y. Yamamoto, *Nat. Phys.* **2014**, *10*, 803.
- [158] S. Ghosh, T. C. H. Liew, *npj Quantum Inf.* **2020**, *6*, 16.
- [159] H. Deng, H. Haug, Y. Yamamoto, *Rev. Mod. Phys.* **2010**, *82*, 1489.
- [160] R. Su, J. Wang, J. Zhao, J. Xing, W. Zhao, C. Diederichs, T. C. H. Liew, Q. Xiong, *Sci. Adv.* **2018**, *4*, eaau0244.
- [161] R. Su, S. Ghosh, J. Wang, S. Liu, C. Diederichs, T. C. H. Liew, Q. Xiong, *Nat. Phys.* **2020**, *16*, 301.
- [162] F. P. Laussy, A. V. Kavokin, I. A. Shelykh, *Phys. Rev. Lett.* **2010**, *104*, 106402.
- [163] S. Kim, B. Zhang, Z. Wang, J. Fischer, S. Brodbeck, M. Kamp, C. Schneider, S. Höfling, H. Deng, *Phys. Rev. X* **2016**, *6*, 011026.
- [164] A. Amo, T. C. H. Liew, C. Adrados, R. Houdré, E. Giacobino, A. V. Kavokin, A. Bramati, *Nat. Photonics* **2010**, *4*, 361.
- [165] X. Xu, S. Jin, *Sci. Adv.* **2020**, *6*, eaab3095.
- [166] L. C. Flatten, S. Christodoulou, R. K. Patel, A. Buccheri, D. M. Coles, B. P. L. Reid, R. A. Taylor, I. Moreels, J. M. Smith, *Nano Lett.* **2016**, *16*, 7137.
- [167] H. Deng, G. Weihs, D. Snoke, J. Bloch, Y. Yamamoto, *Proc. Natl. Acad. Sci. U. S. A.* **2003**, *100*, 15318.
- [168] R. Su, C. Diederichs, J. Wang, T. C. H. Liew, J. Zhao, S. Liu, W. Xu, Z. Chen, Q. Xiong, *Nano Lett.* **2017**, *17*, 3982.
- [169] A. Amo, J. Lefrère, S. Pigeon, C. Adrados, C. Ciuti, I. Carusotto, R. Houdré, E. Giacobino, A. Bramati, *Nat. Phys.* **2009**, *5*, 805.
- [170] G. Lerario, A. Fieramosca, F. Barachati, D. Ballarini, K. S. Daskalakis, L. Dominici, M. De Giorgi, S. A. Maier, G. Gigli, S. Kéna-Cohen, D. Sanvitto, *Nat. Phys.* **2017**, *13*, 837.
- [171] A. Maître, G. Lerario, A. Medeiros, F. Claude, Q. Glorieux, E. Giacobino, S. Pigeon, A. Bramati, *Phys. Rev. X* **2020**, *10*, 041028.
- [172] L. A. Smirnov, D. A. Smirnova, E. A. Ostrovskaya, Y. S. Kivshar, *Phys. Rev. B: Condens. Matter Mater. Phys.* **2014**, *89*, 235310.
- [173] T. Boulier, M. J. Jacquet, A. Maître, G. Lerario, F. Claude, S. Pigeon, Q. Glorieux, A. Bramati, E. Giacobino, A. Amo, J. Bloch, *Adv. Quantum Technol.* **2020**, *3*, 2000052.
- [174] G. Tosi, G. Christmann, N. G. Berloff, P. Tsotsis, T. Gao, Z. Hatzopoulos, P. G. Savvidis, J. J. Baumberg, *Nat. Phys.* **2012**, *8*, 190.
- [175] A. Amo, D. Sanvitto, F. P. Laussy, D. Ballarini, E. Del Valle, M. D. Martin, A. Lemaître, J. Bloch, D. N. Krizhanovskii, M. S. Skolnick, C. Tejedor, L. Viña, *Nature* **2009**, *457*, 291.
- [176] T. Boulier, M. J. Jacquet, A. Maître, G. Lerario, F. Claude, S. Pigeon, Q. Glorieux, A. Amo, J. Bloch, A. Bramati, E. Giacobino, *Adv. Quantum Technol.* **2020**, *3*, 2000052.
- [177] A. Fieramosca, L. Polimeno, V. Ardizzone, L. De Marco, M. Pugliese, V. Maiorano, M. De Giorgi, L. Dominici, G. Gigli, D. Gerace, D. Ballarini, D. Sanvitto, *Sci. Adv.* **2019**, *5*, eaav9967.
- [178] J. Wu, S. Ghosh, R. Su, A. Fieramosca, T. C. H. Liew, Q. Xiong, *Nano Lett.* **2021**, *21*, 3120.
- [179] T. Lecomte, V. Ardizzone, M. Abbarchi, C. Diederichs, A. Miard, A. Lemaître, I. Sagnes, P. Senellart, J. Bloch, C. Delalande, J. Tignon, P. Roussignol, *Phys. Rev. B: Condens. Matter Mater. Phys.* **2013**, *87*, 155302.
- [180] Q. Shang, M. Li, L. Zhao, D. Chen, S. Zhang, S. Chen, P. Gao, C. Shen, J. Xing, G. Xing, B. Shen, X. Liu, Q. Zhang, *Nano Lett.* **2020**, *20*, 6636.
- [181] S. Zhang, Q. Shang, W. Du, J. Shi, Z. Wu, Y. Mi, J. Chen, F. Liu, Y. Li, M. Liu, Q. Zhang, X. Liu, *Adv. Opt. Mater.* **2018**, *6*, 1701032.
- [182] T. J. S. Evans, A. Schlaus, Y. Fu, X. Zhong, T. L. Atallah, M. S. Spencer, L. E. Brus, S. Jin, X. Y. Zhu, *Adv. Opt. Mater.* **2018**, *6*, 1700982.
- [183] S. Fan, J. D. Joannopoulos, *Phys. Rev. B: Condens. Matter Mater. Phys.* **2002**, *65*, 235112.
- [184] T. Fujita, Y. Sato, T. Kuitani, T. Ishihara, *Phys. Rev. B: Condens. Matter Mater. Phys.* **1998**, *57*, 12428.
- [185] S. C. Malek, A. C. Overvig, S. Shrestha, N. Yu, *Nanophotonics* **2021**, *10*, 655.
- [186] T. Karzig, C. E. Bardyn, N. H. Lindner, G. Refael, *Phys. Rev. X* **2015**, *5*, 031001.
- [187] W. Liu, Z. Ji, Y. Wang, G. Modi, M. Hwang, B. Zheng, V. J. Sorger, A. Pan, R. Agarwal, *Science* **2020**, *370*, 600.
- [188] K. Koshelev, A. Bogdanov, Y. Kivshar, *Opt. Photonics News* **2020**, *31*, 38.
- [189] A. S. Solntsev, G. S. Agarwal, Y. S. Kivshar, *Nat. Photonics* **2021**, *15*, 327.
- [190] A. Amo, J. Bloch, *C. R. Phys.* **2016**, *17*, 934.
- [191] I. M. Georgescu, S. Ashhab, F. Nori, *Rev. Mod. Phys.* **2014**, *86*, 153.
- [192] A. Amo, in *CLEO: Science and Innovations 2014*, OSA Technical Digest (online), Optical Society of America, **2014**, paper STu3O.1; https://doi.org/10.1364/CLEO_SI.2014.STu3O.1.
- [193] V. G. Sala, D. D. Solnyshkov, I. Carusotto, T. Jacqmin, A. Lemaître, H. Terças, A. Nalitov, M. Abbarchi, E. Galopin, I. Sagnes, J. Bloch, G. Malpuech, A. Amo, *Phys. Rev. X* **2015**, *5*, 011034.
- [194] M. Abbarchi, A. Amo, V. G. Sala, D. D. Solnyshkov, H. Flayac, L. Ferrier, I. Sagnes, E. Galopin, A. Lemaître, G. Malpuech, J. Bloch, *Nat. Phys.* **2013**, *9*, 275.
- [195] L. Balents, *Nature* **2010**, *464*, 199.
- [196] D. C. Tsui, H. L. Stormer, A. C. Gossard, *Phys. Rev. Lett.* **1982**, *48*, 1559.
- [197] Y. Cao, V. Fatemi, S. Fang, K. Watanabe, T. Taniguchi, E. Kaxiras, P. Jarillo-Herrero, *Nature* **2018**, *556*, 43.

- [198] F. Baboux, L. Ge, T. Jacqmin, M. Biondi, E. Galopin, A. Lemaître, L. Le Gratiet, I. Sagnes, S. Schmidt, H. E. Türeci, A. Amo, J. Bloch, *Phys. Rev. Lett.* **2016**, *116*, 066402.
- [199] M. Goda, S. Nishino, H. Matsuda, *Phys. Rev. Lett.* **2006**, *96*, 126401.
- [200] V. Goblot, B. Rauer, F. Vicentini, A. Le Boité, E. Galopin, A. Lemaître, L. Le Gratiet, A. Harouri, I. Sagnes, S. Ravets, C. Ciuti, A. Amo, J. Bloch, *Phys. Rev. Lett.* **2019**, *123*, 113901.
- [201] J. Wang, J. Yang, T. J. Alexander, Y. S. Kivshar, *Phys. Rev. A: At., Mol., Opt. Phys.* **2009**, *79*, 043610.
- [202] T. J. Alexander, E. A. Ostrovskaya, Y. S. Kivshar, *Phys. Rev. Lett.* **2006**, *96*, 040401.
- [203] T. Jacqmin, I. Carusotto, I. Sagnes, M. Abbarchi, D. D. Solnyshkov, G. Malpuech, E. Galopin, A. Lemaître, J. Bloch, A. Amo, *Phys. Rev. Lett.* **2014**, *112*, 116402.
- [204] C. E. Whittaker, E. Cancellieri, P. M. Walker, D. R. Gulevich, H. Schomerus, D. Vaitiekus, B. Royall, D. M. Whittaker, E. Clarke, I. V. Iorsh, I. A. Shelykh, M. S. Skolnick, D. N. Krizhanovskii, *Phys. Rev. Lett.* **2018**, *120*, 097401.
- [205] P. St-Jean, V. Goblot, E. Galopin, A. Lemaître, T. Ozawa, L. L. Gratiet, I. Sagnes, J. Bloch, A. Amo, *Nat. Photonics* **2017**, *11*, 651.
- [206] M. Dusel, S. Betzold, O. A. Egorov, S. Klembt, J. Ohmer, U. Fischer, S. Höfling, C. Schneider, *Nat. Commun.* **2020**, *11*, 2863.
- [207] A. Ryou, D. Rosser, A. Saxena, T. Fryett, A. Majumdar, *Phys. Rev. B* **2018**, *97*, 235307.
- [208] G. Muñoz-Matutano, A. Wood, M. Johnsson, X. Vidal, B. Q. Baragiola, A. Reinhard, A. Lemaître, J. Bloch, A. Amo, G. Nogues, B. Besga, M. Richard, T. Volz, *Nat. Mater.* **2019**, *18*, 213.
- [209] V. Shahnazaryan, I. A. Shelykh, O. Kyriienko, *Phys. Rev. B* **2016**, *93*, 245302.
- [210] M. Achermann, J. A. Hollingsworth, V. I. Klimov, *Phys. Rev. B* **2003**, *68*, 245302.
- [211] M. Saba, S. Minniberger, F. Quochi, J. Roither, M. Marceddu, A. Gocalinska, M. V. Kovalenko, D. V. Talapin, W. Heiss, A. Mura, G. Bongiovanni, *Adv. Mater.* **2009**, *21*, 4942.
- [212] A. Piryatinski, S. A. Ivanov, S. Tretiak, V. I. Klimov, *Nano Lett.* **2007**, *7*, 108.
- [213] F. Rajadell, J. I. Climente, J. Planelles, *Phys. Rev. B* **2017**, *96*, 035307.
- [214] K. De Greve, L. Yu, P. L. McMahon, J. S. Pelc, C. M. Natarajan, N. Y. Kim, E. Abe, S. Maier, C. Schneider, M. Kamp, S. Höfling, R. H. Hadfield, A. Forchel, M. M. Fejer, Y. Yamamoto, *Nature* **2012**, *491*, 421.
- [215] W. B. Gao, P. Fallahi, E. Togan, J. Miguel-Sanchez, A. Imamoglu, *Nature* **2012**, *491*, 426.
- [216] J. R. Schaibley, A. P. Burgers, G. A. McCracken, L. M. Duan, P. R. Berman, D. G. Steel, A. S. Bracker, D. Gammon, L. J. Sham, *Phys. Rev. Lett.* **2013**, *110*, 167401.
- [217] A. Imamoglu, D. D. Awschalom, G. Burkard, D. P. DiVincenzo, D. Loss, M. Sherwin, A. Small, *Phys. Rev. Lett.* **1999**, *83*, 4204.
- [218] D. M. Lukin, C. Dory, M. A. Guidry, K. Y. Yang, S. D. Mishra, R. Trivedi, M. Radulaski, S. Sun, D. Vercrusse, G. H. Ahn, J. Vučković, *Nat. Photonics* **2020**, *14*, 330.
- [219] J. M. Kindem, A. Ruskuc, J. G. Bartholomew, J. Rochman, Y. Q. Huan, A. Faraon, *Nature* **2020**, *580*, 201.
- [220] S. Chen, M. Raha, C. M. Phenicie, S. Ourari, J. D. Thompson, *Science* **2020**, *370*, 592.
- [221] P. Jobez, C. Laplane, N. Timoney, N. Gisin, A. Ferrier, P. Goldner, M. Afzelius, *Phys. Rev. Lett.* **2015**, *114*, 230502.
- [222] N. E. Kopteva, E. Kirstein, E. A. Zhukov, M. Hussain, A. S. Bhatti, A. Pawlis, D. R. Yakovlev, M. Bayer, A. Greilich, *Phys. Rev. B* **2019**, *100*, 205415.
- [223] G. Blasse, *Prog. Solid State Chem.* **1988**, *18*, 79.
- [224] T. Zhong, P. Goldner, *Nanophotonics* **2019**, *8*, 2003.
- [225] J. E. McPeak, S. S. Eaton, G. R. Eaton, in *Rare-Earth Element Biochemistry: Characterization and Applications of Lanthanide-Binding Biomolecules* (Ed: J. A. Cotruvo), *Methods in Enzymology*, Vol. 651, Academic Press, Cambridge, Massachusetts **2021**, pp. 63–101.
- [226] R. M. Macfarlane, *J. Lumin.* **2002**, *100*, 1.
- [227] W. Tittel, M. Afzelius, T. Chanelière, R. L. Cone, S. Kröll, S. A. Moiseev, M. Sellars, *Laser Photonics Rev.* **2010**, *4*, 244.
- [228] C. W. Thiel, T. Bttger, R. L. Cone, *J. Lumin.* **2011**, *131*, 353.
- [229] C. O'Brien, N. Lauk, S. Blum, G. Morigi, M. Fleischhauer, *Phys. Rev. Lett.* **2014**, *113*, 063603.
- [230] L. A. Williamson, Y. H. Chen, J. J. Longdell, *Phys. Rev. Lett.* **2014**, *113*, 203601.
- [231] I. Craiciu, M. Lei, J. Rochman, J. G. Bartholomew, A. Faraon, *Optica* **2021**, *8*, 114.
- [232] S. Chen, S. Ourari, M. Raha, C. M. Phenicie, M. T. Uysal, J. D. Thompson, *Opt. Express* **2021**, *29*, 4902.
- [233] M. Raha, S. Chen, C. M. Phenicie, S. Ourari, A. M. Dibos, J. D. Thompson, *Nat. Commun.* **2020**, *11*, 1605.
- [234] B. Merkel, A. Ulanowski, A. Reiserer, *Phys. Rev. X* **2020**, *10*, 041025.
- [235] R. W. Equall, Y. Sun, R. L. Cone, R. M. MacFarlane, *Phys. Rev. Lett.* **1994**, *72*, 2179.
- [236] J. G. Bartholomew, J. Rochman, T. Xie, J. M. Kindem, A. Ruskuc, I. Craiciu, M. Lei, A. Faraon, *Nat. Commun.* **2020**, *11*, 3266.
- [237] M. Afzelius, C. Simon, H. De Riedmatten, N. Gisin, *Phys. Rev. A: At., Mol., Opt. Phys.* **2009**, *79*, 052329.
- [238] A. Kinos, D. Hunger, R. Kolesov, K. Mølmer, H. de Riedmatten, P. Goldner, A. Tallaire, L. Morvan, P. Berger, S. Welinski, K. Karrai, L. Rippe, S. Kröll, A. Walther, arXiv:2103.15743v1, **2021**.
- [239] T. J. Milstein, D. M. Kroupa, D. R. Gamelin, *Nano Lett.* **2018**, *18*, 3792.
- [240] X. Huang, S. Han, W. Huang, X. Liu, *Chem. Soc. Rev.* **2013**, *42*, 173.
- [241] C. S. Erickson, M. J. Crane, T. J. Milstein, D. R. Gamelin, *J. Phys. Chem. C* **2019**, *123*, 12474.
- [242] J. Y. D. Roh, M. D. Smith, M. J. Crane, D. Biner, T. J. Milstein, K. W. Krämer, D. R. Gamelin, *Phys. Rev. Mater.* **2020**, *4*, 105405.
- [243] D. Serrano, K. S. Kumar, B. Heinrich, O. Fuhr, D. Hunger, M. Ruben, P. Goldner, arXiv:2105.07081v1, **2021**.
- [244] J. Tribollet, J. Behrends, K. Lips, *EPL* **2008**, *84*, 20009.
- [245] K. Bader, D. Dengler, S. Lenz, B. Endeward, S. D. Jiang, P. Neugebauer, J. Van Slageren, *Nat. Commun.* **2014**, *5*, 5304.
- [246] H. J. Von Bardeleben, S. A. Zargaleh, J. L. Cantin, W. B. Gao, T. Biktatirov, U. Gerstmann, *Phys. Rev. Mater.* **2019**, *3*, 124605.
- [247] R. Beaulac, P. I. Archer, X. Liu, S. Lee, G. M. Salley, M. Dobrowolska, J. K. Furdyna, D. R. Gamelin, *Nano Lett.* **2008**, *8*, 1197.
- [248] R. Beaulac, L. Schneider, P. I. Archer, G. Bacher, D. R. Gamelin, *Science* **2009**, *325*, 973.
- [249] S. T. Ochsenein, D. R. Gamelin, *Nat. Nanotechnol.* **2011**, *6*, 112.
- [250] H. D. Nelson, L. R. Bradshaw, C. J. Barrows, V. A. Vlaskin, D. R. Gamelin, *ACS Nano* **2015**, *9*, 11177.
- [251] A. M. Schimpf, S. T. Ochsenein, D. R. Gamelin, *J. Phys. Chem. Lett.* **2015**, *6*, 457.
- [252] M. Bello, G. Platero, J. I. Cirac, A. González-Tudela, *Sci. Adv.* **2019**, *5*, eaaw0297.
- [253] B. M. Anderson, R. Ma, C. Owens, D. I. Schuster, J. Simon, *Phys. Rev. X* **2016**, *6*, 041043.
- [254] E. Kim, X. Zhang, V. S. Ferreira, J. Banker, J. K. Iverson, A. Sipahigil, M. Bello, A. González-Tudela, M. Mirhosseini, O. Painter, *Phys. Rev. X* **2021**, *11*, 011015.
- [255] M. J. Hartmann, *J. Opt.* **2016**, *18*, 104005.
- [256] S. Mittal, V. V. Orre, G. Zhu, M. A. Gorlach, A. Poddubny, M. Hafezi, *Nat. Photonics* **2019**, *13*, 692.
- [257] A. Saxena, Y. Chen, Z. Fang, A. Majumdar, arXiv:2106.14325v1, **2021**.



Yueyang Chen earned his Ph.D. degree in Electrical Engineering at the University of Washington. His Ph.D. research primarily focuses on coupling solution-processed material and 2D materials to nanophotonic devices. The goal of his research is to enable scalable photonic devices for both classical and quantum applications.



David Sharp is currently a Physics Ph.D. student at the University of Washington. His research primarily focuses on coupling solution-processed semiconductor nanocrystals to dielectric nanocrystals. The goal of his research is to enable scalable photonic devices based on low-power optical nonlinearities.



Abhi Saxena is a Ph.D. student in the Department of Electrical & Computer Engineering at the University of Washington, Seattle. In 2017, he worked for a brief period as a researcher on quantum networks using optical links at IQST, University of Calgary. He received his bachelor's degree in Electrical Engineering from Indian Institute of Technology, Delhi in 2018. His current research focuses on developing nanophotonic coupled cavity systems for quantum simulation.



Hao Nguyen obtained his B. S. in Chemistry from Texas A&M University in 2020. Currently, he is pursuing his Ph.D. in Chemistry at the University of Washington under the guidance of Professor Brandi Cossairt. His research focuses on the synthesis and fabrication of giant and high quantum yield colloidal quantum dots for solid-state lighting and photonics applications.



Brandi Cossairt received her B.S. in Chemistry from the California Institute of Technology in 2006 and her Ph.D. from the Massachusetts Institute of Technology in 2010. She then trained as an NIH NRSA Postdoctoral Fellow at Columbia University before joining the Department of Chemistry at the University of Washington in 2012. Her research group examines the nucleation, growth, surface chemistry, and reactivity of nanoscale materials to enable next-generation technologies in the diverse areas of displays, lighting, catalysis, quantum information, and hybrid matter.



Arka Majumdar is an Associate Professor in the departments of Electrical and Computer Engineering and Physics at the University of Washington. He received B. Tech. from IIT-Kharagpur (2007), where he was honored with the President's Gold Medal. He completed his MS (2009) and Ph.D. (2012) in Electrical Engineering at Stanford University. He spent one year at the University of California, Berkeley (2012–2013) as a postdoc before joining Intel Labs (2013–2014). His research interests include developing a hybrid nanophotonic platform using emerging material systems for optical information science, imaging, and microscopy.